

Y3.N21/5:6/1275

GOVT. DOC.

NATIONAL ADVISORY COMMITTEE FOR AERONAUTICS

TECHNICAL NOTE

No. 1275

A LIFTING-SURFACE-THEORY SOLUTION AND TESTS OF AN ELLIPTIC
TAIL SURFACE OF ASPECT RATIO 3 WITH A
0.5-CHORD 0.85-SPAN ELEVATOR

By Robert S. Swanson, Stewart M. Crandall, and Sadie Miller

Langley Memorial Aeronautical Laboratory
Langley Field, Va.



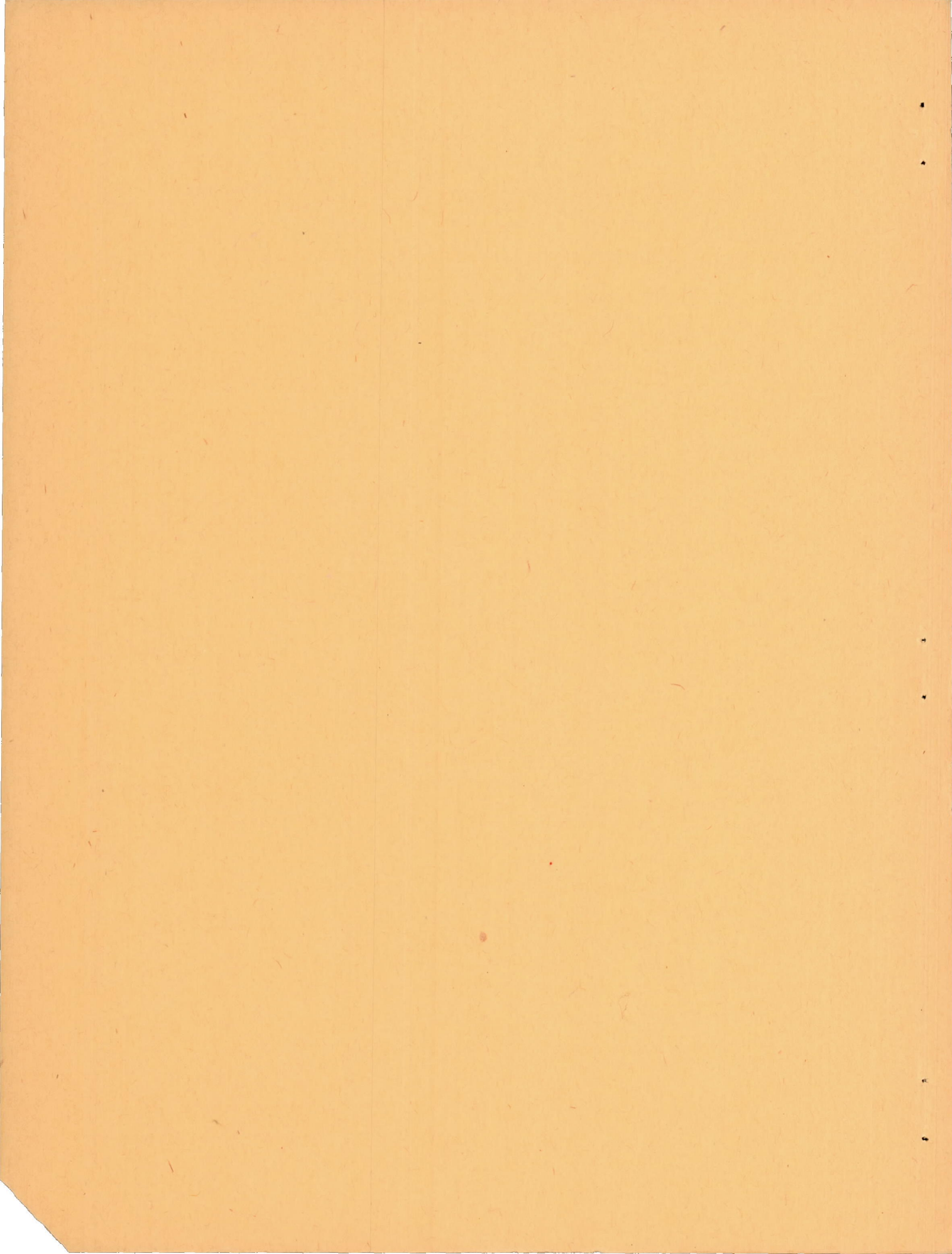
Washington

May 1947

~~CONF. STATE LIBRARY~~

MAY 7 1947

BUSINESS, SCIENCE
& TECHNOLOGY DEPARTMENT



NATIONAL ADVISORY COMMITTEE FOR AERONAUTICS

TECHNICAL NOTE NO. 1275

A LIFTING-SURFACE-THEORY SOLUTION AND TESTS OF AN ELLIPTIC
TAIL SURFACE OF ASPECT RATIO 3 WITH A
0.5 CHORD 0.85-SPAN ELEVATOR

By Robert S. Swanson, Stewart M. Crandall, and Sadie Miller

SUMMARY

An electromagnetic-analogy model of the vortex load, estimated from lifting-line theory with an arbitrary fairing near the elevator tip, on a thin elliptic horizontal tail surface of aspect ratio 3 with a 0.5-chord 0.85-span plain elevator was constructed and tested. The aspect-ratio corrections to the lift and hinge moments were calculated from the measured results.

A comparison of the aspect-ratio corrections for the partial-span elevators was made with those previously presented for full-span elevators. The comparison indicates that the incremental difference in the lift parameters between the full-span and the partial-span elevators may be estimated satisfactorily by lifting-line theory. The incremental difference for the curve of hinge-moment coefficient against angle of attack is usually small. Only about 10 percent of the incremental difference for the slope of the curve of hinge-moment coefficient against elevator deflection is given by lifting-line theory; the total lifting-surface-theory increment is -0.0009 per degree for the configuration considered.

Wind-tunnel results for a tail surface of the same plan form are presented. The differences in estimated lifting-surface aspect-ratio corrections for the full-span and the partial-span cases were checked satisfactorily by the experimental data. A few tests with a cut-out for the rudder were also presented. The effects of the cut-out on the hinge-moment characteristics were large.

INTRODUCTION

A method was presented in reference 1 for estimating the finite-span values of the lift and hinge-moment parameters of full-span

elevators from the section data. The present investigation was undertaken in order to provide some data from which the lift and hinge-moment parameters for partial-span elevators could be estimated. The case presented is that of a thin elliptic horizontal tail surface of aspect ratio 3 with a 0.5-chord 0.85-span plain elevator.

References 1 and 2 showed that it is necessary to use lifting-surface-theory aspect-ratio corrections to estimate satisfactorily the finite-span hinge-moment parameters. Lifting-surface-theory solutions are usually determined by a rapidly converging process of successive approximations, of which the first approximation is the lifting-line-theory solution. For partial-span elevators or flaps, however, the contour lines of constant circulation strength (see references 3 and 4) calculated by means of lifting-line theory have abrupt discontinuities near the elevator tip, as shown by the contour lines of the circulation function $\frac{\Gamma}{\Gamma_{\max}}$ in figure 1. Since

such sharp bends in the contour lines are smoothed out by aerodynamic induction, a more satisfactory loading may be obtained for the next approximation by arbitrarily fairing the contour lines so that they are smooth in the region just upstream of the elevator tip. The contour lines on the elevator itself are smooth and therefore need not be altered. In order to obtain some idea of the best means of accomplishing this fairing, the three-dimensional pressure-distribution data of reference 5 for a rectangular wing with partial-span split flaps were integrated to obtain contour lines of constant circulation strength. For comparison, the contour lines for the experimental span loading, divided into flap-type and angle-of-attack-type loadings (reference 6) by use of the principles of lifting-line theory, were also constructed. Both sets of contour lines are given in figure 2. In figure 3 are presented the contour lines of figure 1 refaired similarly to the contour lines of the experimental data presented in figure 2.

An electromagnetic-analogy model having the contour lines of figure 3 was then constructed and tested. The incremental lifting-surface-theory aspect-ratio corrections were determined by calculating the increments of chordwise and spanwise loading that would result for a lifting surface shaped to correspond to the difference between the measured downwash and the downwash determined from the two-dimensional theories for the same contour pattern (fig. 3). In the calculation of the increments of the lift and hinge-moment parameters (additional aspect-ratio corrections), the difference between the downwash measured for the faired contour pattern of figure 3 and the downwash calculated from the 2 two-dimensional theories for the same contour pattern are assumed to be nearly equal to the corresponding

difference in the measured and calculated downwash for the contour pattern of figure 1.

In order to provide an experimental check of the aspect-ratio corrections, some wind-tunnel tests were made of a model of the same plan form and of NACA 0009 airfoil section, with both full-span and partial-span elevators. The results, together with some additional data showing the effect of elevator cut-outs, are presented in appendix A.

The hinge-moment corrections for "feeler ailerons" (small-span wide-chord ailerons at the wing tips) designed to provide the stick feel for thin-plate, retractable-type, lateral-control devices are of current interest. In order to provide some data for these arrangements, the hinge-moment aspect-ratio corrections for a 0.5-chord 0.15-span feeler aileron on a wing of aspect ratio 3 are briefly summarized in appendix B.

SYMBOLS

Γ	circulation strength
C_L	lift coefficient
c_l	section lift coefficient
c_h	section hinge-moment coefficient
C_h	hinge-moment coefficient
a_0	section slope of lift curve, per radian
α	angle of attack
α_e	effective angle of attack, radians $\left(\frac{c_l}{a_0}\right)$
α_0	two-dimensional angle of attack
δ	elevator deflection

δ_t	tab deflection
w	vertical component of induced velocity
E	Jones edge-velocity correction factor for lift (reference 7)
E_{ef}	effective edge-velocity correction for lift of elliptic wing with partial-span flap (see references 1 and 7)
V	free-stream velocity
x	chordwise distance from wing leading edge
x_o	chordwise distance from wing leading edge to point at which downwash is desired
y	spanwise distance from plane of symmetry
c	chord
c_s	center-section chord
\bar{c}_e	root-mean-square chord of elevator
b	span of tail
ϕ	trailing-edge angle, degrees
q	dynamic pressure
S	area of tail
b_e	span of elevator
A	aspect ratio (b^2/S)
F	hinge-moment factor for theoretical load caused by streamline-curvature correction (reference 1)
η	experimentally determined reduction factor for F to include the effects of viscosity (reference 1)
Δ	increment
Δ'	increment of parameter; value for elevator with full-span flap minus value for elevator with partial-span flap

Δ'' increment of parameter; value for elevator with no cut-out
minus value for elevator with cut-out

Parameters:

$$c_{l\alpha} \quad \left(\frac{\partial c_l}{\partial \alpha_0} \right)_{\delta} = a_0$$

$$c_{l\delta} \quad \left(\frac{\partial c_l}{\partial \delta} \right)_{\alpha_0}$$

$$\left(\alpha_0 \right)_{c_l} \quad \left| \left(\frac{\partial \alpha_0}{\partial \delta} \right)_{c_l} \right| = \frac{\left(\frac{\partial c_l}{\partial \delta} \right)_{\alpha_0}}{\left(\frac{\partial c_l}{\partial \alpha} \right)_{\delta}}$$

$$\left(\alpha_0 \right)_{c_L} \quad \left| \left(\frac{\partial \alpha}{\partial \delta} \right)_{c_L} \right| = \frac{\left(\frac{\partial c_L}{\partial \delta} \right)_{\alpha}}{\left(\frac{\partial c_L}{\partial \alpha} \right)_{\delta}}$$

$$c_{h\delta} \quad \left(\frac{\partial c_{h_e}}{\partial \delta} \right)_{\alpha, \delta_t}$$

$$c_{h\alpha} \quad \left(\frac{\partial c_{h_e}}{\partial \alpha} \right)_{\delta, \delta_t}$$

The subscript outside the parenthesis indicates the factor held constant in determining the parameter.

Subscripts:

LL lifting-line theory

LIM modified lifting-line theory

LS lifting-surface theory

strip strip

max maximum

TE trailing edge

e elevator or effective

f flap

δ	elevator-deflection-type load
α	angle-of-attack-type load
$\Delta\alpha_i$	incremental induced angle-of-attack-type load
i	induced
SC	streamline curvature

Angular measures are in radians in the text and in degrees in appendixes A and B and table I unless specified otherwise.

ELECTROMAGNETIC-ANALOGY MODEL

Lifting-line-theory vortex pattern.- The vortex pattern for an elliptic tail surface of aspect ratio 3 at zero angle of attack with a 0.5-chord 0.85-span elevator deflected is desired. In order to determine the vortex pattern, it is necessary to know the span load distribution as estimated from lifting-line theory and the chord load distribution as estimated from thin-airfoil theory.

The span load distribution for an elliptic wing having an aspect ratio of 3 and a section slope of the lift curve of 2π per radian and with 0.85-span elevator was determined quite accurately from unpublished influence lines similar to those of reference 8, but calculated for elliptic wings. The span load distribution, in terms of the parameter $\frac{c\alpha_e}{c_s\alpha}$, is given in figure 4.

The chordwise circulation function $\frac{2\Gamma}{c\alpha V}$ must be known for both a flat plate at an angle of attack and a flat plate at zero angle of attack with a 0.5-chord elevator deflected. The mathematical expressions for these functions are given in references 3 and 9, and curves of the functions as estimated from thin-airfoil theory are presented in figure 5.

In order to construct the vortex pattern, it is necessary to determine how much of the load $\left(\frac{c\alpha_e}{c_s\alpha} \text{ of fig. 4}\right)$ at each section is elevator-type loading and how much is angle-of-attack-type loading. According to the assumptions of lifting-line theory, the amount of elevator-type loading is that given by strip theory; that is, this

loading is equal to the two-dimensional loading with aerodynamic induction neglected. The induced loading is entirely angle-of-attack-type loading and is equal to the loading obtained by strip theory minus the actual resultant loading given in figure 4.

The strip-theory loading over the elevator span in terms of the parameter $\frac{c\alpha_e}{c_s\alpha}$ is equal to $\frac{c}{c_s}$ (see fig. 4) since $\alpha_e = \alpha$ by definition. The circulation strength of elevator-type loading therefore is equal to $\left(\frac{2\Gamma}{cc_lV}\right)_\delta \frac{c}{c_s}$. The circulation strength of angle-of-attack-type loading is then equal to $\left(\frac{2\Gamma}{cc_lV}\right)_\alpha \left(\frac{c}{c_s} - \frac{c\alpha_e}{c_s\alpha}\right)$. If all values of circulation strength are divided by the maximum value at the wing center section, the values of Γ/Γ_{\max} at any spanwise station $\frac{y}{b/2}$ and at any chordwise station x/c can be determined from figures 4 and 5 by the formulas that follow. For values of $\frac{y}{b/2}$ from 0 to 0.85,

$$\frac{\Gamma}{\Gamma_{\max}} = \frac{\left(\frac{2\Gamma}{cc_lV}\right)_\delta \frac{c}{c_s} - \left(\frac{2\Gamma}{cc_lV}\right)_\alpha \left(\frac{c}{c_s} - \frac{c\alpha_e}{c_s\alpha}\right)}{\left(\frac{2\Gamma}{c_s c_l V}\right)_{\max}} \quad (1a)$$

For values of $\frac{y}{b/2}$ from 0.85 to 1.0,

$$\frac{\Gamma}{\Gamma_{\max}} = \frac{\left(\frac{2\Gamma}{cc_lV}\right)_\alpha \left(\frac{c\alpha_e}{c_s\alpha}\right)}{\left(\frac{2\Gamma}{c_s c_l V}\right)_{\max}} \quad (1b)$$

Contour lines of $\frac{\Gamma}{\Gamma_{\max}}$ determined from equations (1) for this configuration are given in figure 1.

Modified lifting-line-theory vortex pattern.- As stated in the "Introduction," it is desirable to fair the contour lines arbitrarily in the region just ahead of the elevator tip in order to simplify the construction of the model and to account approximately for the known smoothing effects of aerodynamic induction. The fairing over the region occupied by the elevator was not altered. The contour lines of figure 3 were obtained by fairing the curves of figure 1 similarly to the contour lines of figure 2. The contour lines of figure 3 were then used as the first approximation to the circulation strength (called modified lifting-line-theory loading).

Construction of Model

An electromagnetic-analogy model (fig. 6) of the loading represented by the contour lines of figure 3 was constructed and tested. The model was constructed of 100 wires representing the incremental vortices. The wires used were B. & S. No. 15 gage (0.057 in. diam.) copper. The span of the model was 100 inches, and the wake extended 2.4 semispans from the leading edge of the root section. The test setup, measuring equipment, and methods were similar to those described in reference 4.

LIFTING-SURFACE-THEORY CALCULATIONS FOR DOWNWASH

Because the additional lifting-surface-theory plan-form corrections are determined from the difference between the actual downwash measurements and the values estimated by lifting-line and thin-airfoil theories, it is necessary to calculate the downwash from these two-dimensional theories, as well as to measure the downwash for the electromagnetic-analogy model.

Downwash Calculated by Two-Dimensional Theories

Lifting-line-theory loading.- The downwash given by the 2 two-dimensional theories corresponding to the lifting-line-theory loading is, of course, equal to the geometric slope of the surface times the free-stream velocity. This value of downwash is everywhere zero except over the elevator itself. Over the elevator the downwash is equal to δV where

$$\delta = \frac{1}{(\alpha\delta)c_l} \frac{c_l}{c_l\alpha} = \frac{c_l}{c_l\delta}$$

and

$$c_l = \frac{2\Gamma_{\text{strip}}}{cV}$$

$$= \frac{2\Gamma_{\text{TE}}}{cV} \frac{\alpha}{\alpha_e}$$

and therefore

$$w_\delta = \delta V$$

$$= \frac{2\Gamma_{\text{TE}} \alpha}{(\alpha_\delta)_{c_l} c_l \alpha_e c}$$

The downwash in terms of a nondimensional parameter is thus

$$\left(\frac{wb}{2\Gamma_{\text{max}}} \right)_\delta = \frac{2}{\frac{c}{b/2} \left(\frac{c\alpha_e}{c_s \alpha} \right)_{\text{max}} (\alpha_\delta)_{c_l} c_l \alpha_e} \quad (2)$$

since

$$\Gamma_{\text{max}} = \Gamma_{\text{TE}}$$

and

$$\frac{c\alpha_e}{c_s \alpha} = \frac{\alpha_e}{\alpha}$$

where

$$c_s = c$$

From figure 4, $\left(\frac{c\alpha_e}{c_s \alpha} \right)_{\text{max}} = 0.59$; for a thin airfoil, $c_l \alpha = 2\pi$;

for $\frac{c_e}{c} = 0.5$, $(\alpha_\delta)_{c_l} = \frac{\pi + 2}{2\pi}$; and for an elliptic wing of

$A = 3$, $\frac{c_s}{b/2} = \frac{8}{3\pi}$. The increment of downwash over the flap there-

fore is $\left(\frac{wb}{2\Gamma_{\text{max}}} \right)_\delta = 0.778$.

The downwash corresponding to the spanwise distribution of Γ_{TE} is just neutralized by the downwash corresponding to the bound vorticity of the induced load (of angle-of-attack type). This downwash must be calculated, however, in order to determine the modified lifting-line-theory downwash.

The downwash resulting from aerodynamic induction is equal to $\alpha_1 V$ or $(\alpha - \alpha_e) V$. Over the sections of the model within the elevator span, $\alpha = \delta(\alpha_\delta)_{c_l}$; and over the section outboard of the elevator, $\alpha = 0$. For all sections

$$\alpha_e = \frac{2\Gamma_{TE}}{c_l \alpha c V}$$

since

$$\Gamma_{TE} = \frac{c c_l V}{2} = \frac{c_l \alpha_e c V}{2}$$

The induced downwash over the span of the elevator is thus

$$\left(\frac{wb}{2\Gamma_{max}}\right)_{i_{LL}} = \left(\frac{wb}{2\Gamma_{max}}\right)_\delta (\alpha_\delta)_{c_l} - \frac{1}{\pi \left(\frac{c}{b/2}\right) \left(\frac{c\alpha_e}{c_s \alpha}\right)_{max}} \frac{c\alpha_e}{c_s \alpha} \quad (3)$$

and over the sections outboard at the elevator is

$$\begin{aligned} \left(\frac{wb}{2\Gamma_{max}}\right)_{i_{LL}} &= - \frac{1}{\pi \left(\frac{c}{b/2}\right) \left(\frac{c\alpha_e}{c_s \alpha}\right)_{max}} \frac{c\alpha_e}{c_s \alpha} \\ &= - \frac{A}{8 \left(\frac{c}{c_s}\right) \left(\frac{c\alpha_e}{c_s \alpha}\right)_{max}} \end{aligned} \quad (4)$$

These downwash parameters are plotted in figure 7.

Modified lifting-line-theory loading.- The additional aspect-ratio corrections are determined from the difference between the measured lifting-surface-theory downwash and the downwash calculated from the two-dimensional theories for the modified lifting-line-theory loading. The downwash corresponding to the arbitrary fairing of the contour lines (fig. 3) must therefore be calculated by the two-dimensional theories. Because the span loading was not changed by the arbitrary fairing, the component of downwash corresponding to the spanwise distribution of Γ_{TE} (equations (3) and (4)) is unchanged. The chordwise distribution between the stations $\frac{y}{b/2} = 0.70$ and $\frac{y}{b/2} = 0.95$ was altered.

The procedure used in calculating the chordwise distribution of the downwash was to plot the magnitude of the altered contour lines against the chordwise position in a form similar to figure 5. The curve of Γ/Γ_{max} thus obtained can be integrated by means of the Biot-Savart law to obtain the downwash at any point x_0 as follows:

$$\frac{wb}{2\Gamma_{max}} = \frac{1}{2\pi} \int_0^{\frac{c}{b/2}} \frac{1}{\left(\frac{x}{b/2} - \frac{x_0}{b/2}\right)} \frac{d(\Gamma/\Gamma_{max})}{\frac{dx}{b/2}} \frac{dx}{b/2} \quad (5)$$

The curve of Γ/Γ_{max} was integrated by assuming that each small segment of the curve could be approximated satisfactorily by a parabola, a procedure similar to that presented in reference 3.

The sum of the downwash due to the bound vorticity Γ/Γ_{max} given by equation (5) and the downwash induced by the spanwise distribution of Γ_{TE} (equations (3) and (4)) gives the incremental downwash caused by modifying the contour lines of figure 1. The incremental values with the geometric downwash give the total modified lifting-line-theory downwash.

Values of nondimensional downwash for the first-approximation or modified lifting-line-theory loading are presented in figure 8. The downwash curves are rather irregular, as might be expected, since the fairing of the curve of Γ/Γ_{max} was done entirely arbitrarily and any slight errors in this curve show up to a very magnified scale in the downwash curves.

Downwash Measurements from Electromagnetic-Analogy Model

The magnetic-field strength of the electromagnetic-analogy model was measured at four or five vertical heights, 25 spanwise stations, and from 25 to 60 chordwise stations. A number of repeat tests were made to check the accuracy of the measurements, and satisfactory checks were obtained.

The measured data were faired, extrapolated to zero vertical height, and converted to the nondimensional downwash function $\left(\frac{wb}{2\Gamma_{\max}}\right)_{LS}$ as discussed in reference 4. Corrections for the finite length of the trailing vortex sheet were calculated and applied as indicated in reference 4. The final curves of $\left(\frac{wb}{2\Gamma_{\max}}\right)_{LS}$ for the two semispans were then averaged and are presented in figure 9.

Incremental Values of Downwash

In figure 10 are presented the incremental values of the nondimensional downwash $\Delta\left(\frac{wb}{2\Gamma_{\max}}\right)_{LS}$ as determined by taking the difference between the lifting-surface-theory values of figure 9 and the values obtained by the two-dimensional theories for the modified lifting-line-theory loading of figure 8.

DEVELOPMENT OF ASPECT-RATIO CORRECTION FORMULA

General Procedure

The incremental lifting-surface-theory aspect-ratio corrections are determined by calculating the increments of chordwise and spanwise loadings that would result from a lifting surface shaped to correspond to the differences between the lifting-surface-theory downwash and the downwash determined from the two-dimensional theories, that is, the loadings of a lifting surface with shape given by letting the slope of the surface equal the downwash distribution of figure 10.

Because the incremental aspect-ratio corrections are reasonably small, approximate formulas are usually used to evaluate them. The methods and formulas usually used are given in reference 1 and include first-order compressibility corrections (reference 10). Some preliminary computations were made by more exact methods for the present case, in which the downwash near the elevator tip is so irregular. These preliminary computations indicated that the corrections would

not be given with satisfactory accuracy unless the actual chordwise variation in downwash was used. The following formulas are therefore developed by use of thin-airfoil-theory methods (references 11 and 12).

The following development of the aspect-ratio corrections was made by means of incompressible-flow relations. First-order compressibility corrections may be estimated by use of the linear perturbation theory of reference 10 as was done in reference 1.

Lift

The incremental correction to the lift of an elliptic tail surface is

$$\Delta C_L = \frac{4}{\pi} \frac{A}{AE + 2} \frac{2\Gamma_{\max}}{bV} \int_0^{1.0} \frac{\frac{\Delta c_l}{2\Gamma_{\max}} \frac{c}{c_s}}{\frac{bV}{bV}} d\left(\frac{y}{b/2}\right) \quad (6)$$

where values of the parameter $\frac{\Delta c_l}{\frac{2\Gamma_{\max}}{bV}}$ are obtained from the data presented in figure 10 through the use of the relationship

$$\frac{\Delta c_l}{\frac{2\Gamma_{\max}}{bV}} = 4 \int_0^{1.0} \Delta \left(\frac{wb}{2\Gamma_{\max}} \right)_{LS} \sqrt{\frac{x/c}{1 - \frac{x}{c}}} d\frac{x}{c} \quad (7)$$

derived from thin-airfoil theory. (See equation (25) of chapter IV of reference 11.)

Evaluation of $(\Delta C_{L\delta})_{LS}$ requires an estimation of the relation between Γ_{\max} and the elevator deflection δ . In accordance with lifting-line theory, $\left(\frac{c\alpha_e}{c_s\alpha} \right)_{\max} = 0.59$. (See fig. 4 for this particular wing-flap combination.)

Thus,

$$\alpha_e = 0.59\alpha$$

$$\alpha = 0.59(\alpha_\delta)_{c_l} \delta$$

$$\alpha_e = 0.59\left(\frac{\pi + 2}{2\pi}\right) \delta$$

and

$$\Gamma_{\max_{LL}} = \frac{c_s c_l V}{2} = \frac{c_s V}{2} 2\pi\alpha_e = c_s V \delta (1.517) \quad (8)$$

In reference 1 are given values of the ratio

$$\left[\frac{(\alpha_\delta)_{c_L}}{(\alpha_\delta)_{c_l}} \right]_{LS}$$

for full-span elevators. If the assumption is made that this correction is approximately proportional to the elevator span and if the Jones edge-velocity correction is applied, a more nearly correct relation between Γ_{\max} and δ can be obtained from the following approximation:

$$\Gamma_{\max} = \Gamma_{\max_{LL}} \frac{A + 2}{AE + 2} \left(\left\{ \left[\frac{(\alpha_\delta)_{c_L}}{(\alpha_\delta)_{c_l}} \right]_{LS} - 1 \right\} \frac{b_e}{b} + 1 \right) \quad (9)$$

or

$$\frac{2\Gamma_{\max}}{bV} = \frac{1.517 \times 8}{A\pi} \frac{A + 2}{AE + 2} \left(\left\{ \left[\frac{(\alpha_\delta)_{c_L}}{(\alpha_\delta)_{c_l}} \right]_{LS} - 1 \right\} \frac{b_e}{b} + 1 \right) \delta \quad (10)$$

and

$$(\Delta C_{L6})_{LS} = \frac{48.5}{\pi^2} \frac{A+2}{(AE+2)^2} \left(\left\{ \frac{[(\alpha_6) c_L]}{[(\alpha_6) c_L]_{LS}} - 1 \right\} \frac{b_e}{b} + 1 \right) \int_0^{1.0} \frac{\Delta c_l}{2\Gamma_{\max}} \frac{c}{c_s} d\left(\frac{y}{b/2}\right) \quad (11)$$

Therefore

$$(\Delta C_{L6})_{LS} = 0.855 \int_0^{1.0} \frac{\Delta c_l}{2\Gamma_{\max}} \frac{c}{c_s} d\left(\frac{y}{b/2}\right)$$

For the present case of a horizontal tail of aspect ratio 3, with a 0.5-chord 0.85-span plain elevator

$$\begin{aligned} (\Delta C_{L6})_{LS} &= 0.855 \times 0.41 \\ &= 0.35 \end{aligned} \quad (12)$$

The lifting-line-theory value of C_{L6} for an elliptic wing with a partial-span constant-percentage-chord elevator is given by

$$(C_{L6})_{LL} = \frac{8A(\alpha_6) c_l \int_0^{b_e/b} \frac{c}{c_s} d\left(\frac{y}{b/2}\right)}{A+2} \quad (13)$$

for a lift-curve slope of 2π .

For the wing under discussion with a value of $(\alpha_6) c_l$ of $\frac{\pi+2}{2\pi}$

$$(C_{L6})_{LL} = 2.87$$

and

$$(C_{L6})_{LS} = (C_{L6})_{LL} - (\Delta C_{L6})_{LS} = 2.52$$

If it is assumed that the concept of an effective edge-velocity correction (see reference 1) can be used in the partial-span-flap case, then

$$(C_{L\delta})_{LS} = \frac{0.93 \times 2\pi(\alpha\delta)_{c_l} A}{AE_{ef} + 2} = \frac{0.93(\pi + 2)A}{AE_{ef} + 2} = 2.52$$

which gives for E_{ef} a value of 1.23. Thus, for section slopes of the lift curve not equal to 2π , the following assumption may be made:

$$(C_{L\delta})_{LS} = \frac{0.93c_{l\alpha}(\alpha\delta)_{c_l}}{E_{ef} + \frac{c_{l\alpha}}{\pi A}} \quad (14)$$

Hinge Moment

Determination of $(C_{h\delta})_{LS}$.—The lifting-surface-theory hinge-moment parameter $(C_{h\delta})_{LS}$ is given by the expression

$$(C_{h\delta})_{LS} = (C_{h\delta})_{LL} + (\Delta C_{h\delta})_{LS} \quad (15)$$

Because the contour lines over the elevator were not altered from those computed for the lifting-line-theory load, the lifting-line-theory value of the hinge-moment coefficient for the modified load is identical with that for the unmodified load. This value is

$$(C_{h\delta})_{LL} = c_{h\delta} - c_{h\alpha} \frac{(c_e/c)^2}{(\bar{c}_e/c_s)^2} \frac{b_e}{b} \int_0^{b_e/b} \left[\frac{\left(\frac{wb}{2\Gamma_{max}}\right)_{iLL}}{0.778} \right]_{LL} \left(\frac{c}{c_s}\right)^2 d\left(\frac{y}{b/2}\right) \quad (16)$$

From the wing geometry

$$\frac{(c_e/c)^2}{(\bar{c}_e/c_s)^2 \frac{b_e}{b}} = 1.55$$

From the downwash curves of figure 7 the integral may be evaluated as 0.2215. This evaluation assumes the span-load curve to be unchanged by small changes in the slope of the lift curve. Equation (15) may be written as

$$(C_{h\delta})_{LS} = c_{h\delta} - 0.344c_{h\alpha} + (\Delta C_{h\delta})_{LS} \quad (17)$$

The lifting-surface-theory correction to the slope of the hinge moment against elevator deflection $(\Delta C_{h\delta})_{LS}$ is equal to the hinge moment of a 50-percent-chord elevator on a surface, which is given by the difference in the measured downwash and the lifting-line-theory downwash (fig. 10). Over most of the wing, the difference in downwash is equivalent to a parabolic-arc-camber airfoil at an angle of attack.

The hinge-moment corrections are computed by thin-airfoil-theory formula in two parts (see reference 1) as follows:

$$(\Delta C_{h\delta})_{LS} = (\Delta C_{h\delta})_{\Delta\alpha_i} + (\Delta C_{h\delta})_{SC} \quad (18)$$

The increment $(\Delta C_{h\delta})_{\Delta\alpha_i}$ is obtained from the induced downwash at the 0.5-chord point. The increment $(\Delta C_{h\delta})_{SC}$ is not a streamline-curvature correction in the sense used in reference 1, since the downwash curves near the outboard end of the flap define a somewhat irregular surface, not a parabolic-arc surface. The hinge-moment corrections estimated by the two methods, although appreciable, are not too great; therefore, for the purpose of simplifying the system of notation and in order that the viscosity efficiency factor η for parabolic-arc airfoils can be used for the present case, the symbol $(\Delta C_{h\delta})_{SC}$ is used to

identify the part of the correction not given by $(\Delta C_{h\delta})_{\Delta\alpha_1}$. The numerical values of $(\Delta C_{h\delta})_{SC}$ are computed, however, for the actual distorted surface.

The induced-angle-of-attack correction is

$$(\Delta C_{h\delta})_{\Delta\alpha_1} = -c_{h\alpha} \frac{A}{AE + 2} \frac{(c_e/c)^2}{\frac{b_e}{b} (\bar{c}_e/c_s)^2} \int_0^{b_e/b} \frac{\Delta\alpha_1}{\delta} \left(\frac{c}{c_s}\right)^2 d\left(\frac{y}{b/2}\right) \quad (19)$$

If the value of $\Delta\alpha_1$ is given in terms of the increment of downwash parameter at the $c/2$ stations $\Delta \left(\frac{wb}{2\Gamma_{\max}} \right)_{c/2} \frac{2\Gamma_{\max}}{bV}$ and the value of δ is obtained from equation (10), the

following equation is obtained:

$$(\Delta C_{h\delta})_{\Delta\alpha_1} = -c_{h\alpha} \frac{(c_e/c)^2}{\frac{b_e}{b} (\bar{c}_e/c_s)^2} 3.86 \frac{A + 2}{(AE + 2)^2} \left\{ \left[\frac{(\alpha_\delta)_{CL}}{(\alpha_\delta)_{c_l}} - 1 \right] \frac{b_e}{b} + 1 \right\} \int_0^{b_e/b} \Delta \left(\frac{wb}{2\Gamma_{\max}} \right)_{c/2} \left(\frac{c}{c_s}\right)^2 d\left(\frac{y}{b/2}\right) \quad (20)$$

By the use of the data of figure 10 the integral was evaluated; hence

$$(\Delta C_{h\delta})_{\Delta\alpha_1} = -0.017 c_{h\alpha} \quad (21)$$

The value of $(\Delta C_{h\delta})_{SC}$ may be determined from

$$(\Delta C_{h\delta})_{SC} = \frac{2\Gamma_{\max}}{bV\delta} \frac{\left(\frac{c_e}{c}\right)^2}{\frac{b_e}{b} \left(\frac{c_e}{c_s}\right)^2} \int_0^{b_e/b} \frac{\Delta c_h}{2\Gamma_{\max}/bV} \left(\frac{c}{c_s}\right)^2 d\left(\frac{y}{b/2}\right) \quad (22)$$

where values of the parameter $\frac{\Delta c_h}{2\Gamma_{\max}/bV}$ are obtained from the data presented in figure 9 by means of the relation

$$\frac{\Delta c_h}{2\Gamma_{\max}/bV} = \int \left(\frac{\partial c_h}{\partial \delta_t} \right)_{\alpha_0, \delta} d \left[\Delta \left(\frac{wb}{2\Gamma_{\max}} \right) - \Delta \left(\frac{wb}{2\Gamma_{\max}} \right)_{0.5c} \right] \quad (23)$$

Numerical values of the parameter $\left(\frac{\partial c_h}{\partial \delta_t} \right)_{\alpha_0, \delta}$ are presented in

figure 11 for a 0.5-chord plain elevator as calculated from the thin-airfoil-theory formulas of reference 12. For flaps with overhang or internal balances, the changes in the parabolic-arc factor $\frac{F}{(c_e/c)^2}$ of reference 1 with the amount of balance can be used as a fair measure of the changes with overhang of the value of $(\Delta C_{h\delta})_{SC}$ determined from equations (22) and (23).

For a horizontal tail surface of aspect ratio 3, with 0.5-chord 0.85-span plain elevator having an assumed value of $c_{l\alpha} = 2\pi$

$$\text{and } (\alpha\delta)_{c_l} = \frac{\pi + 2}{2\pi}$$

$$(\Delta C_{h\delta})_{SC} = 0.2005 \text{ per radian} \quad (24)$$

The lifting-surface-theory value of the parameter $(C_{h\delta})_{LS}$ is obtained by substitution of values from equations (18), (21), and (24) in equation (17) as follows:

$$(C_{h\delta})_{LS} = c_{h\delta} - 0.361c_{h\alpha} + 0.2005$$

In order to estimate $(C_{h\delta})_{LS}$ for the plan-form corrections from the section data with arbitrary values of $c_{l\alpha}$, $(\alpha\delta)_{c_l}$, $c_{h\alpha}$, and $c_{h\delta}$ the following expression may be used:

$$(C_{h\delta})_{LS} = c_{h\delta} - \frac{1.1(\alpha\delta)_{c_l}}{1 + \frac{3\pi}{c_{l\alpha}}} c_{h\alpha} - 0.0487 \frac{F\eta}{(c_e/c)^2} \frac{(\alpha\delta)_{c_l} c_{l\alpha}}{1 + \frac{c_{l\alpha}}{3\pi}} \quad (25)$$

where $A = 3$, $\eta = 1 - 0.0005 \phi^2$, and values of $\frac{F}{(c_e/c)^2}$ are presented in reference 1.

Determination of $(C_{h\alpha})_{LS}$. - The lifting-surface-theory hinge-moment parameter $(C_{h\alpha})_{LS}$ for an elliptic tail surface with a partial-span constant-percentage-chord elevator may be estimated from the relation

$$(C_{h\alpha})_{LS} = c_{h\alpha} \left(1 - \frac{\alpha_1}{\alpha}\right)_{LS} + \frac{[(\Delta C_{h\alpha})_{SC}]_{\text{Partial-span}}}{[(\Delta C_{h\alpha})_{SC}]_{\text{Full-span}}} [(\Delta C_{h\alpha})_{SC}]_{\text{Full-span}}$$

Values of $\left[(\Delta C_{h\alpha})_{SC} \right]_{\text{Full-span}}$ and $\left(\frac{\alpha_1}{\alpha} \right)_{\text{LS}}$ are presented in reference 1 and values of the ratio $\frac{\left[(\Delta C_{h\alpha})_{SC} \right]_{\text{Partial-span}}}{\left[(\Delta C_{h\alpha})_{SC} \right]_{\text{Full-span}}}$, derived from the curves used in estimating the corrections presented in reference 2, are given in figure 12.

COMPARISON OF LIFTING-SURFACE-THEORY RESULTS WITH WIND-TUNNEL DATA

The difference between the aspect-ratio corrections for full-span elevators and partial-span elevators can be determined from the wind-tunnel data presented in appendix A for a condition directly comparable to the case considered in the present paper

($A = 3$, elliptic plan form, $\frac{c_e}{c} = 0.5$, and $\frac{b_e}{b} = 0.85$). In reference 1, some difficulty was encountered in checking the accuracy of the theoretical aspect-ratio corrections against experimental wind-tunnel data because of the scarcity of comparable section and finite-span data. Even the slight surface irregularities obtained in construction of two different models caused large enough changes in the measured hinge moments so that the accuracy of the theoretical aspect-ratio corrections was difficult to evaluate. The accuracy of checking the difference in the corrections for the full-span elevator and the partial-span elevator, however, should be relatively good since the same model was used for both tests, the tip of the elevator being fastened to the elevator in one case and to the stabilizer in the other case.

In table I is presented a summary of the lift and hinge-moment parameters measured from the wind-tunnel data of figure 13 and estimated by means of lifting-line and lifting-surface theories. No values were estimated for the elevator with cut-out. In table II the incremental differences in the parameters for the full-span and the partial-span elevator are given, and in table III the lift and hinge-moment parameters caused by cut-out are given. For the lift parameters both theories predicted approximately the correct increment; however, the slope of the hinge-moment coefficient against elevator deflection estimated by lifting-surface

theory is in much better agreement with the experimental values than the slopes estimated by lifting-line theory.

Only about 10 percent of the incremental difference for the slope of the curve of hinge-moment coefficient against elevator deflection is given by lifting-line theory; the total lifting-surface-theory increment is -0.0009 per degree for the configuration considered herein.

The effects of the cut-out, especially upon the hinge-moment characteristics, were extremely large (see table I) and no adequate theory is available to estimate the effects of the cut-out. In addition, very little experimental section data are available for airfoil sections similar to those at the cut-out. The large effect of the cut-out indicates that lifting-surface-theory solutions such as are given in the present paper and in reference 1 are definitely limited to tail surfaces without cut-outs as well as to small angles of attack and small elevator deflections.

CONCLUDING REMARKS

An electromagnetic-analogy model of the vortex load, estimated from lifting-line theory with an arbitrary fairing near the elevator tip, on a thin elliptic horizontal tail surface of aspect ratio 3 with a 0.5-chord 0.85-span plain elevator was constructed and tested. The aspect-ratio corrections to the lift and hinge moments were calculated from the measured results.

A comparison of the aspect-ratio corrections for the partial-span elevators was made with those previously presented for full-span elevators. The comparison indicates that the incremental difference in the lift parameters between the full-span and the partial-span elevators may be estimated satisfactorily by lifting-line theory. The incremental difference for the curve of hinge-moment coefficient against angle of attack is usually small. Only about 10 percent of the incremental difference for the slope of the curve of hinge-moment coefficient against elevator deflection is given by lifting-line theory; the total lifting-surface-theory increment is -0.0009 per degree for the configuration considered herein.

Wind-tunnel results for a tail surface of the same plan form were presented. The differences in the estimated lifting-surface aspect-ratio corrections for the full-span and partial-span elevators were checked satisfactorily by the experimental data. A few tests with a cut-out for the rudder were also presented. The

effects of the cut-out, especially upon the hinge-moment characteristics, were extremely large and no adequate theory is available to estimate the effects of the cut-out. The large effect of the cut-out indicates that lifting-surface-theory solutions such as are given in the present paper and previously are definitely limited to tail surfaces without cut-outs as well as to small angles of attack and small elevator deflections.

Langley Memorial Aeronautical Laboratory
National Advisory Committee for Aeronautics
Langley Field, Va., August 20, 1946

APPENDIX A

WIND-TUNNEL TESTS

By H. Page Hoggard, Jr.

The test results presented herein were obtained to check the theoretical changes in the aspect-ratio corrections resulting from the use of partial-span elevators. The effect of a rudder cut-out in the elevator was also tested to find out the order of magnitude of such a modification of the elevator.

Apparatus, Model, Corrections, and Tests

All tests were made in the Langley 4- by 6-foot vertical tunnel modified as described in reference 13. The elliptic semispan tail surface (fig. 14) was constructed of laminated mahogany and conformed to the NACA 0009 profile. In the present investigation one elevator with a chord 50 percent of the tail chord was tested. This elevator had a plain radius nose with a gap of 0.5 percent of the airfoil chord. The model was equipped with a removable cut-out block and an elevator tip block so that the four model configurations shown in figure 14 could be obtained. The elevator tip block could be fastened to the elevator or to the main part of the tail surface. The trailing-edge angle of the model measures 11.1° , whereas the theoretical trailing-edge angle (from the published ordinates) measures 11.6° for the NACA 0009 airfoil.

The tail surface was installed as a reflection-plane model by mounting the model with the root section adjacent to one of the tunnel walls. This system is therefore analogous to mounting a 6-foot-span model in an 8- by 6-foot tunnel. The model was supported by the balance frame so that the lift acting on the model could be measured. The gap between the tunnel wall and the root section was about $1/32$ inch.

The greater part of the elevator hinge moment (transmitted through a torque tube) was measured by applying weights at a known lever arm outside the tunnel; the additional increment was measured with a calibrated dial attached to a long flexible torque rod.

Elevator deflections were set with an electric control-surface position indicator.

Each model configuration was tested with the gap open and with the gap sealed. The seal was made of impregnated fabric. The model was tested through an angle-of-attack range of $\pm 20^\circ$ with elevator neutral, and at zero angle of attack through an elevator-deflection range from -5° to 30° .

A dynamic pressure of 13 pounds per square foot, which corresponds to an airspeed of 71 miles per hour at standard sea-level conditions, was maintained for all tests. The test Reynolds number was 1.43×10^6 based on a mean aerodynamic chord of 25.81 inches. The effective Reynolds number (for maximum lift coefficients) was approximately 2.76×10^6 based on a turbulence factor of 1.93 for this tunnel.

No correction was made for leakage around the model support. The following tunnel-wall corrections were added to the data:

$$\Delta\alpha = 2.184 C_{L_T} \text{ (for all four model configurations)}$$

$$\Delta C_{h_1} = 0.0134 C_{L_T} \text{ (full-span elevator without cut-out)}$$

$$\Delta C_{h_1} = 0.0135 C_{L_T} \text{ (full-span elevator with cut-out)}$$

$$\Delta C_{h_1} = 0.0159 C_{L_T} \text{ (partial-span elevator without cut-out)}$$

$$\Delta C_{h_1} = 0.0163 C_{L_T} \text{ (partial-span elevator with cut-out)}$$

where C_{L_T} is the total uncorrected lift coefficient. For methods of calculating corrections for reflection-plane models, see reference 14.

Although the elevator deflection tests were run with the geometric angle of attack at zero, the jet-boundary correction $\Delta\alpha$ given in the foregoing corrections indicates that part of the total lift and elevator hinge moment results from a jet-boundary induced angle of attack. The plots against elevator deflection therefore were made and the slopes were read by using the test data as corrected in the following equations:

$$C_{L_{\text{corrected}}} = C_{L_{\text{uncorrected}}} - \Delta\alpha C_{L_\alpha}$$

$$C_{h_{\text{corrected}}} = C_{h_{\text{uncorrected}}} - \Delta\alpha C_{h_\alpha}$$

$$(\alpha_S) c_{l_{\text{corrected}}} = \frac{C_{L_{\delta_{\text{corrected}}}}}{C_{L_\alpha}}$$

Data

The lift and elevator hinge-moment characteristics of the model tested are presented in figure 13. The various parameters are presented in table I. The slopes were determined for the small angle-of-attack and deflection range.

APPENDIX B

ESTIMATION OF $C_{h\alpha}$ AND $C_{h\delta}$ FOR FEELER AILERONS

Because the aspect-ratio corrections given in the present paper and in reference 1 are obtained from a linear lifting-surface theory, it is possible to superimpose the lifting-surface-theory solutions and thus obtain the solution for 0.5-chord 0.15-span feeler ailerons on a wing of aspect ratio 3. Of course, the arrangement obtained by the use of superposition simulates two ailerons, one on each wing tip, deflected in the same way. A few calculations indicate that the mutual influence of the ailerons upon the hinge-moment characteristics may, however, be safely neglected.

Detailed calculations of the aspect-ratio corrections for this arrangement are not presented because the procedure is similar to that used for the partial-span elevators as given in the main part of the paper.

Because the data are for a rather low aspect ratio for a wing ($A = 3$), the results for the feeler aileron are mainly of comparative value. The incremental difference between the estimated finite-span values and the section values of the hinge-moment parameters (per degree) for the full-span elevator, the 0.85-span elevator, and the 0.15-span feeler aileron are as follows:

Configuration	$\Delta C_{h\alpha}$	$\Delta C_{h\delta}$
Full-span elevator	0.0060	0.0053
0.85-span elevator	.0059	.0062
0.15-span feeler aileron	.0104	.0090

where the section values are

$$C_{h\delta} = -0.014$$

and

$$C_{h\alpha} = -0.0104$$

The aspect-ratio corrections for the case of the feeler aileron are about 70-percent larger than for the case of the full-span elevator. The rather large values of the aspect-ratio corrections are shown especially for the aspect-ratio correction to $C_{h\alpha}$, which is equal to the section value, so that the net value of $C_{h\alpha}$ equals 0.

$C_{h\alpha}$	$C_{h\alpha}$	$C_{h\alpha}$
0.000	0.000	0.000
0.000	0.000	0.000
0.000	0.000	0.000

REFERENCES

1. Swanson, Robert S., and Crandall, Stewart M.: Lifting-Surface-Theory Aspect-Ratio Corrections to the Lift and Hinge-Moment Parameters for Full-Span Elevators on Horizontal Tail Surfaces. NACA TN No. 1175, 1946.
2. Swanson, Robert S., and Gillis, Clarence L.: Limitations of Lifting-Line Theory for Estimation of Aileron Hinge-Moment Characteristics. NACA CB No. 3102, 1943.
3. Cohen, Doris: A Method for Determining the Camber and Twist of a Surface to Support a Given Distribution of Lift. NACA TN No. 855, 1942.
4. Swanson, Robert S., and Crandall, Stewart M.: An Electromagnetic-Analogy Method of Solving Lifting-Surface-Theory Problems. NACA ARR No. L5D23, 1945.
5. Wenzinger, Carl J., and Harris, Thomas A.: Pressure Distribution over a Rectangular Airfoil with a Partial-Span Split Flap. NACA Rep. No. 571, 1936.
6. Allen, H. Julian: Calculation of the Chordwise Load Distribution over Airfoil Sections with Plain, Split, or Serially Hinged Trailing-Edge Flaps. NACA Rep. No. 634, 1938.
7. Jones, Robert T.: Theoretical Correction for the Lift of Elliptic Wings. Jour. Aero. Sci., vol. 9, no. 1, Nov. 1941, pp. 8-10.
8. Pearson, Henry A., and Jones, Robert T.: Theoretical Stability and Control Characteristics of Wings with Various Amounts of Taper and Twist. NACA Rep. No. 635, 1938.
9. Crandall, Stewart M.: Lifting-Surface-Theory Results for Thin Elliptic Wings of Aspect Ratio 3 with Chordwise Loadings Corresponding to 0.5-Chord Plain Flap and to Parabolic-Arc Camber. NACA TN No. 1064, 1946.
10. Goldstein, S., and Young, A. D.: The Linear Perturbation Theory of Compressible Flow, with Applications to Wind-Tunnel Interference. R.&M. No. 1909, British A.R.C., 1943.
11. Munk, Max M.: Fundamentals of Fluid Dynamics for Aircraft Designers. The Ronald Press Co., 1929.

12. Theodorsen, Theodore, and Garrick, I. E.: Nonstationary Flow about a Wing-Aileron-Tab Combination Including Aerodynamic Balance. NACA Rep. No. 736, 1942.
13. Ames, Milton B., Jr., and Sears, Richard I.: Pressure-Distribution Investigation of an N.A.C.A. 0009 Airfoil with a 30-Percent-Chord Plain Flap and Three Tabs. NACA TN No. 759, 1940.
14. Swanson, Robert S., and Toll, Thomas A.: Jet-Boundary Corrections for Reflection-Plane Models in Rectangular Wind Tunnels. NACA ARR No. 3E22, 1943.

TABLE I
PARAMETERS MEASURED FROM WIND-TUNNEL DATA AND CALCULATED FROM THEORETICAL DATA

[Calculations were not made for the arrangements with cut-out because of a lack of comparable section data and theoretical results.]

Lift													
Gap	Cut-out	$C_{L\alpha}$						$C_{L\beta}$					
		Full-span flap			Partial-span flap			Full-span flap			Partial-span flap		
		Measured	Calculated		Measured	Calculated		Measured	Calculated		Measured	Calculated	
			(a)	(b)		(a)	(b)		(a)	(b)		(a)	(b)
Sealed	Without	0.052	0.062	0.053	0.052	0.062	0.053	0.041	0.048	0.042	0.038	0.045	0.040
0.005c	Without	.050	.060	.052	-----	.060	.052	.038	.046	.040	.036	.043	.038
Sealed	With	.049	-----	-----	.047	-----	-----	.031	-----	-----	.028	-----	-----
0.005c	With	.048	-----	-----	.048	-----	-----	.026	-----	-----	.023	-----	-----
Hinge-moment													
Gap	Cut-out	$C_{h\alpha}$						$C_{h\beta}$					
		Full-span flap			Partial-span flap			Full-span flap			Partial-span flap		
		Measured	Calculated		Measured	Calculated		Measured	Calculated		Measured	Calculated	
			(a)	(b)		(a)	(b)		(a)	(b)		(a)	(b)
Sealed	Without	-0.0037	-0.0065	-0.0044	-0.0037	-0.0065	-0.0046	-0.0082	-0.0109	-0.0087	-0.0073	-0.0108	-0.0078
0.005c	Without	-.0043	-.0066	-.0045	-.0042	-.0066	-.0047	-.0078	-.0111	-.0090	-.0068	-.0109	-.0080
Sealed	With	-.0015	-----	-----	-.0013	-----	-----	-.0041	-----	-----	-.0038	-----	-----
0.005c	With	-.0019	-----	-----	-.0015	-----	-----	-.0056	-----	-----	-.0052	-----	-----

^aComputed by lifting-line theory.

^bComputed by lifting-surface theory.

TABLE II
INCREMENTS IN PARAMETERS CAUSED BY PARTIAL SPAN

Gap	Cut-out	$\Delta^{\circ}C_{L\alpha}$			$\Delta^{\circ}C_{L\delta}$			$\Delta^{\circ}C_{h\alpha}$			$\Delta^{\circ}C_{h\delta}$		
		Measured	Calculated		Measured	Calculated		Measured	Calculated		Measured	Calculated	
			(a)	(b)		(a)	(b)		(a)	(b)		(a)	(b)
Sealed	Without	0	0	0	0.003	0.003	0.002	0	0	0.0002	-0.0009	-0.0001	-0.0009
0.005c	Without	0	0	0	.003	.003	.003	-0.0001	0	.0002	-.0010	-.0002	-.0010
Sealed	With	0.002	---	---	.003	-----	-----	-.0002	---	-----	-.0003	-----	-----
0.005c	With	0	---	---	.003	-----	-----	-.0004	---	-----	-.0004	-----	-----

^aComputed by lifting-line theory.

^bComputed by lifting-surface theory.

TABLE III
INCREMENTS IN PARAMETERS CAUSED BY CUT-OUT

Gap	Flap span	$\Delta^{\circ}C_{L\alpha}$	$\Delta^{\circ}C_{L\delta}$	$\Delta^{\circ}C_{h\alpha}$	$\Delta^{\circ}C_{h\delta}$
Sealed	Full	0.003	0.010	-0.0022	-0.0041
0.005c	Full	.002	.012	-.0025	-.0022
Sealed	Partial	.005	.010	-.0021	-.0035
0.005c	Partial	-----	.012	-.0026	-.0016

NATIONAL ADVISORY
COMMITTEE FOR AERONAUTICS

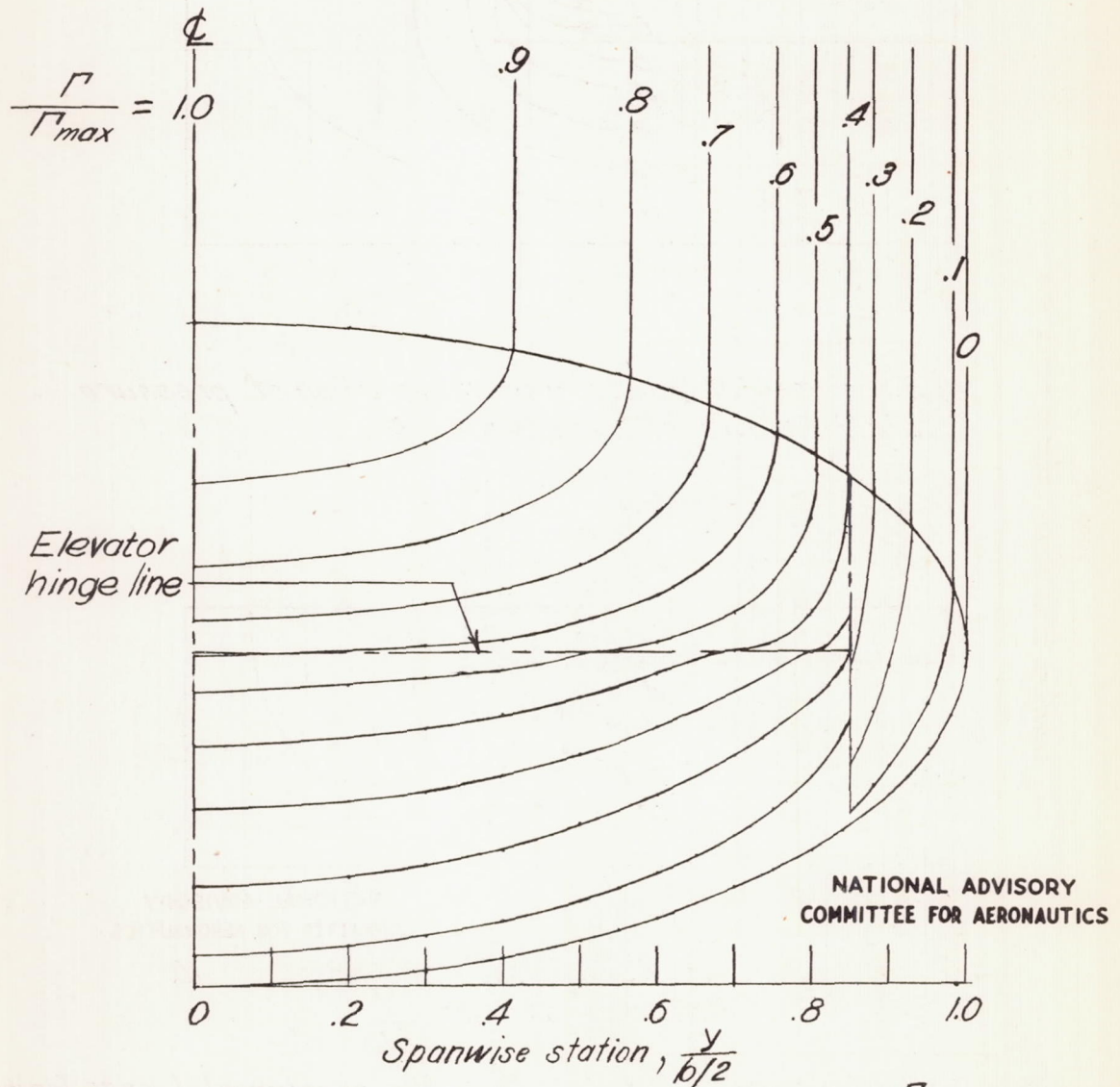
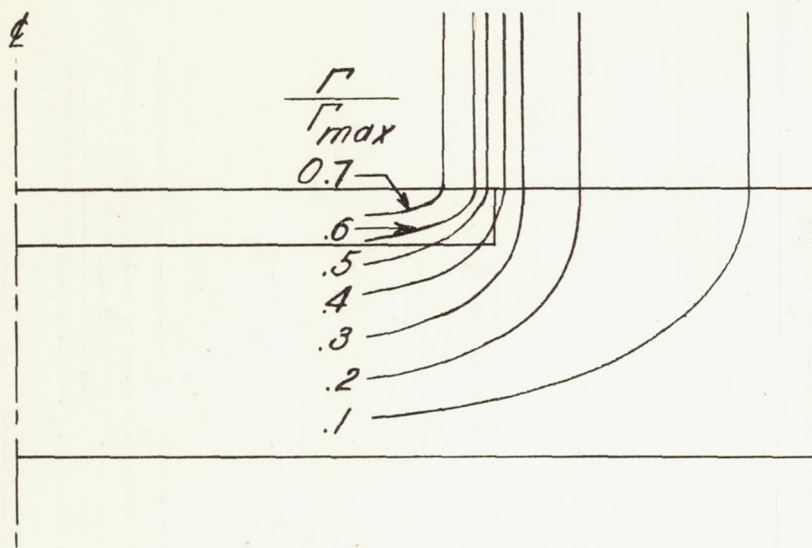
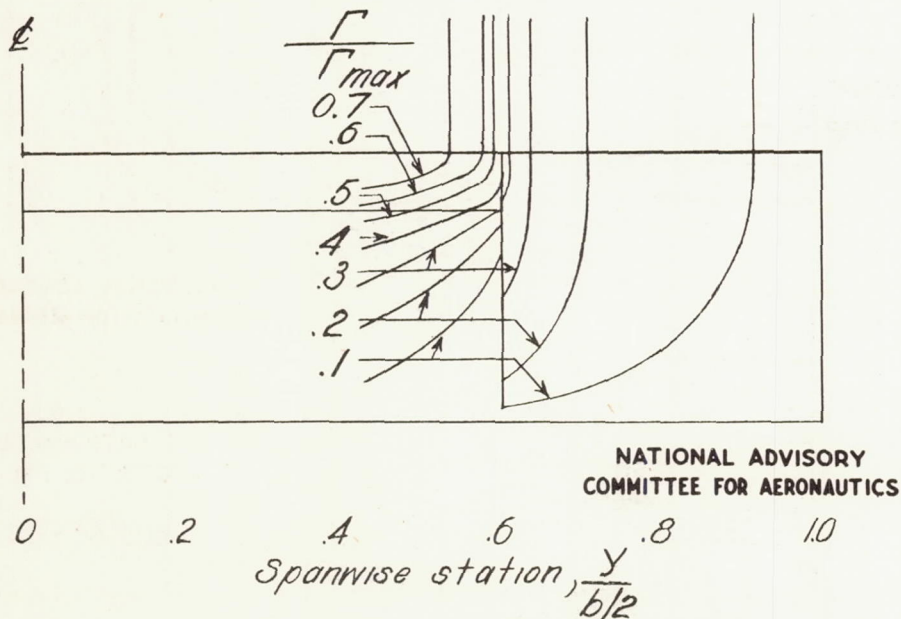


Figure 1.— Contour lines of the circulation function $\frac{\Gamma}{\Gamma_{max}}$ as estimated from thin-airfoil and lifting-line theories for an elliptic wing of aspect ratio 3 with a 0.5-chord 0.85-span plain elevator.



(a) Experimental values from integration of pressure distributions of reference 5.



NATIONAL ADVISORY
COMMITTEE FOR AERONAUTICS

(b) Contour lines computed from the experimental span loading of reference 5 and divided into the experimental chord loadings of reference 6 by means of the assumptions of lifting-line theory.

Figure 2. — Contour lines of the circulation function $\frac{\Gamma}{\Gamma_{max}}$ for a rectangular wing with part-span split flaps. $A=6$; $\frac{b_f}{b} = 0.6$; $\frac{c_f}{c} = 0.2$.

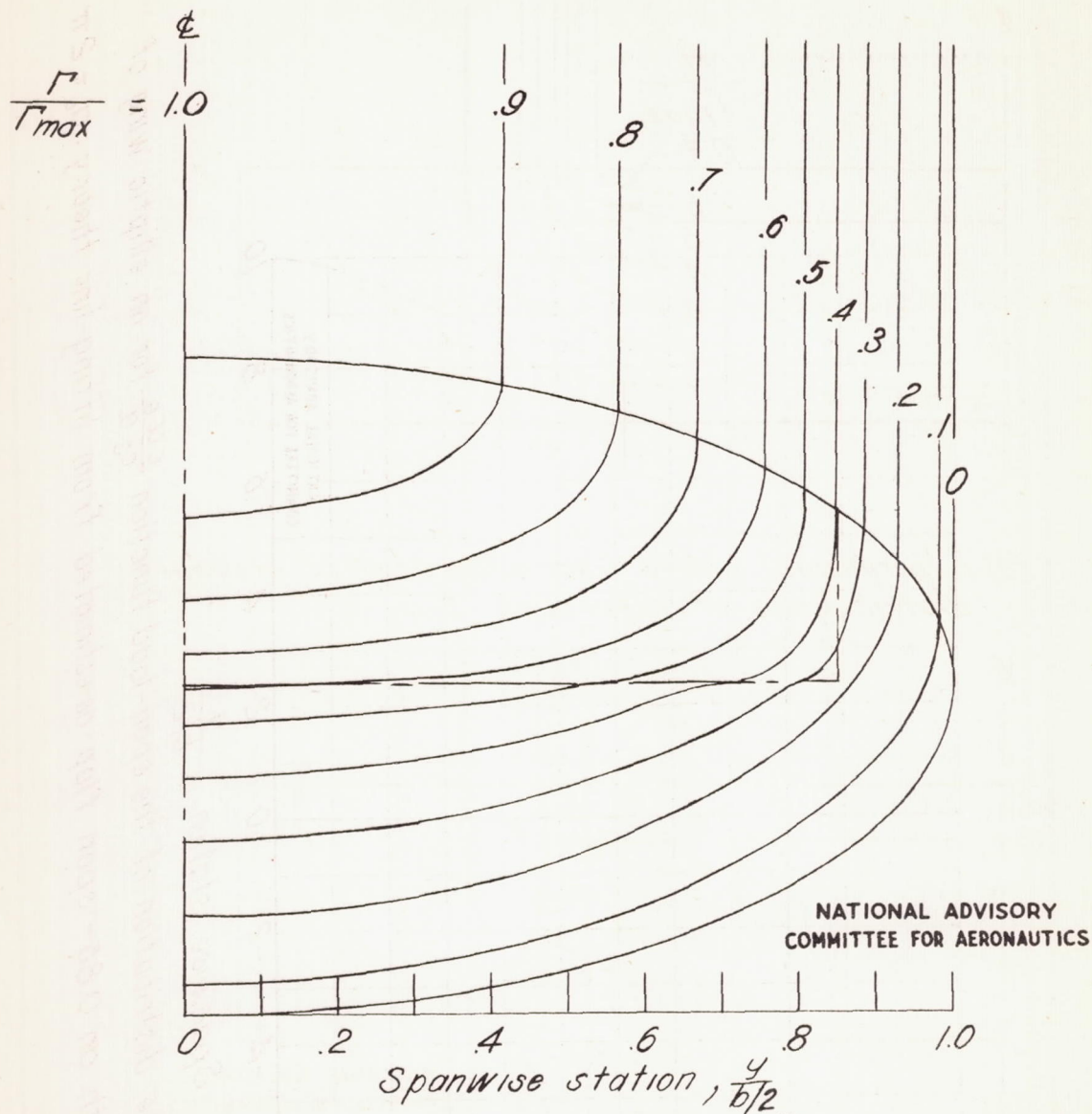


Figure 3. - Contour lines of the circulation function $\frac{\Gamma}{\Gamma_{max}}$ used in constructing an electromagnetic-analogy model of an elliptic wing of aspect ratio 3 with a 0.5-chord 0.85-span elevator. Contour lines are same as those of figure 1 from $0 < \frac{y}{b/2} < 0.7$ with an arbitrary fairing from $0.7 < \frac{y}{b/2} < 1.0$.

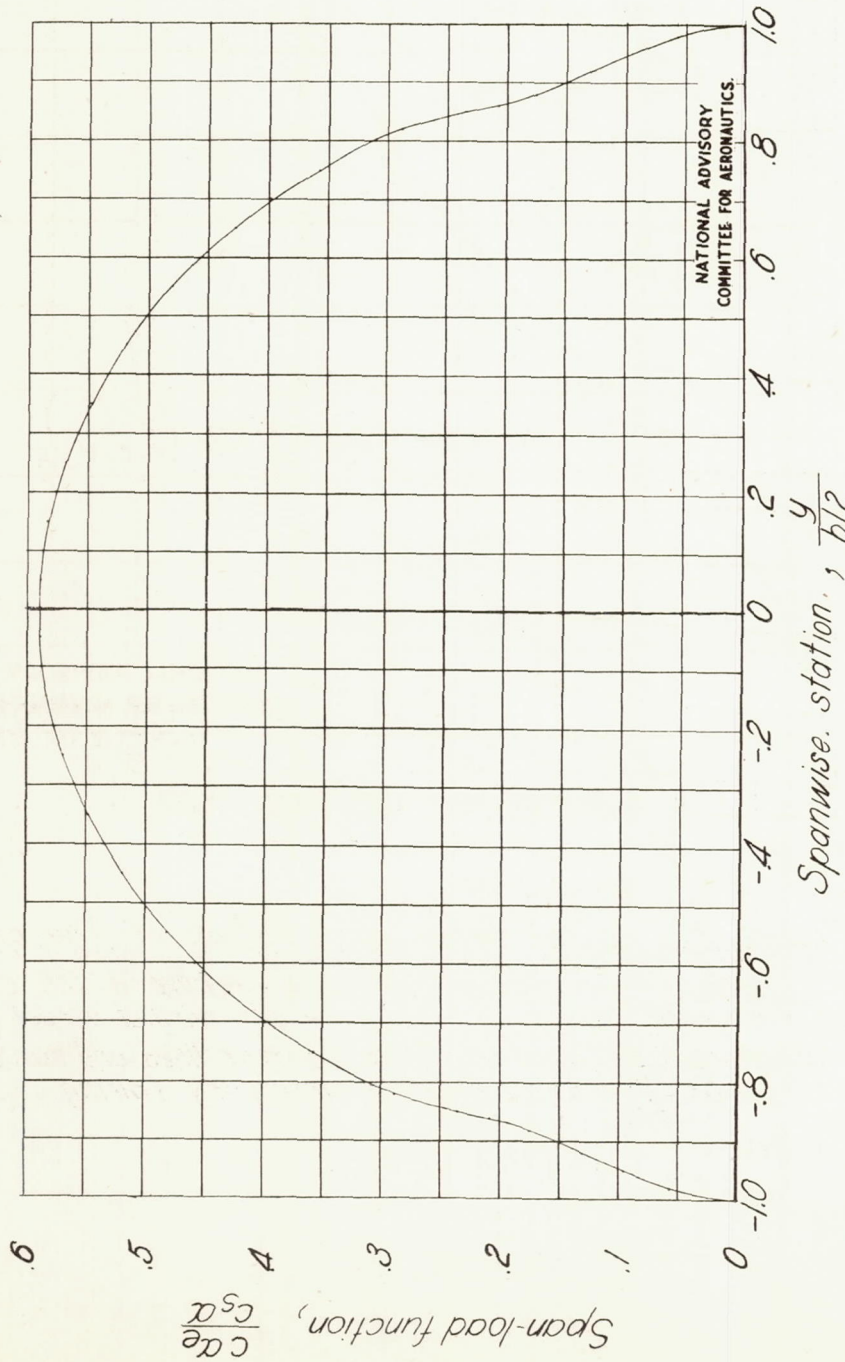


Figure 4. - Spanwise distribution of the span-load function $\frac{c_{l\alpha}}{c_{s\alpha}}$ for an elliptic wing of aspect ratio 3, with an 0.85-span flap as estimated from lifting-line theory. $\alpha_0 = 2\pi$.

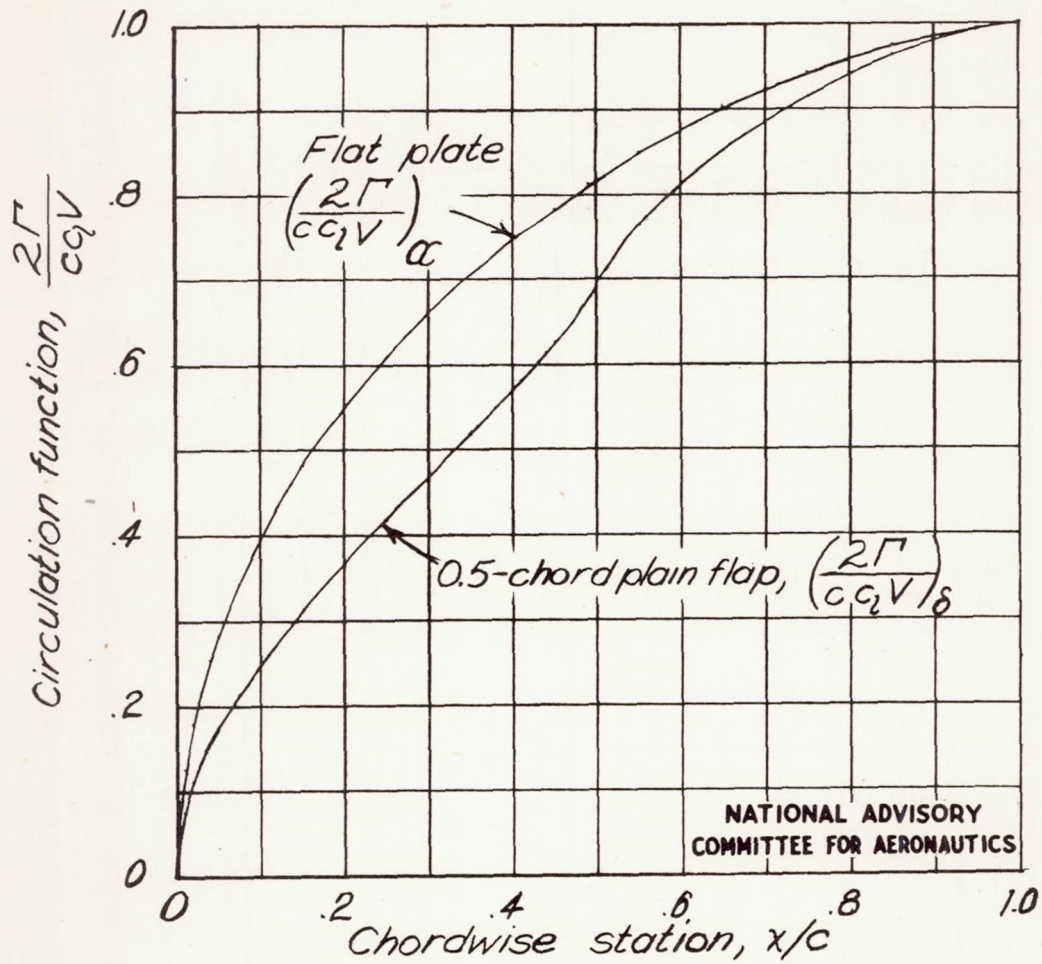


Figure 5 . - Chordwise distribution of the circulation function $\frac{2\Gamma}{c c_2 V}$ for a flat plate and for a 0.5-chord plain flap as estimated from thin-airfoil theory.



Graph of the function $y = 10 - 9e^{-x/10}$

The graph shows the function $y = 10 - 9e^{-x/10}$. The curve starts at the point (0, 1) and increases as x increases, approaching the horizontal asymptote $y = 10$ as $x \rightarrow \infty$.

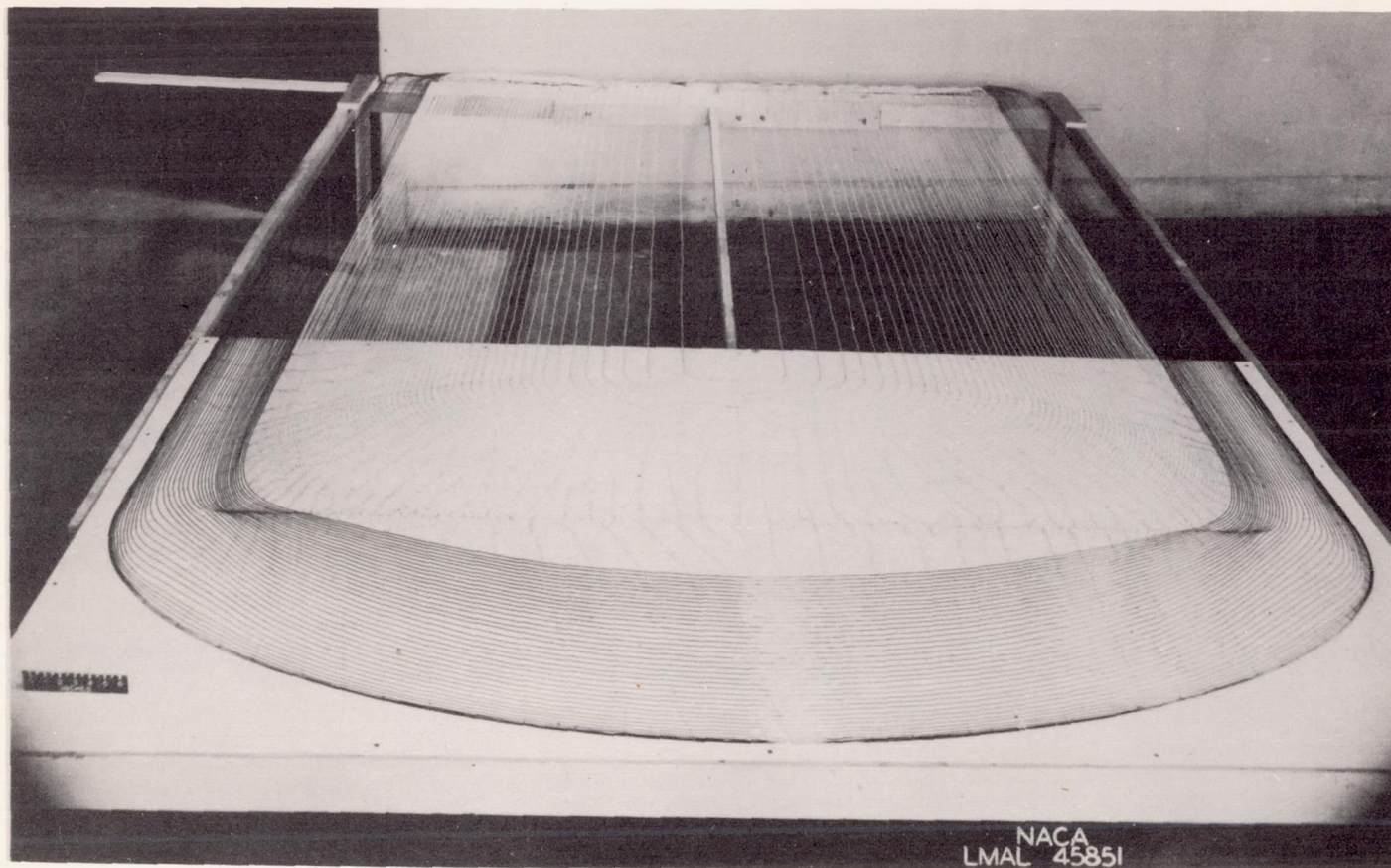


Figure 6.- Electromagnetic-analogy model simulating a thin elliptic tail surface of aspect ratio 3 with a 0.5-chord 0.85-span plain elevator.

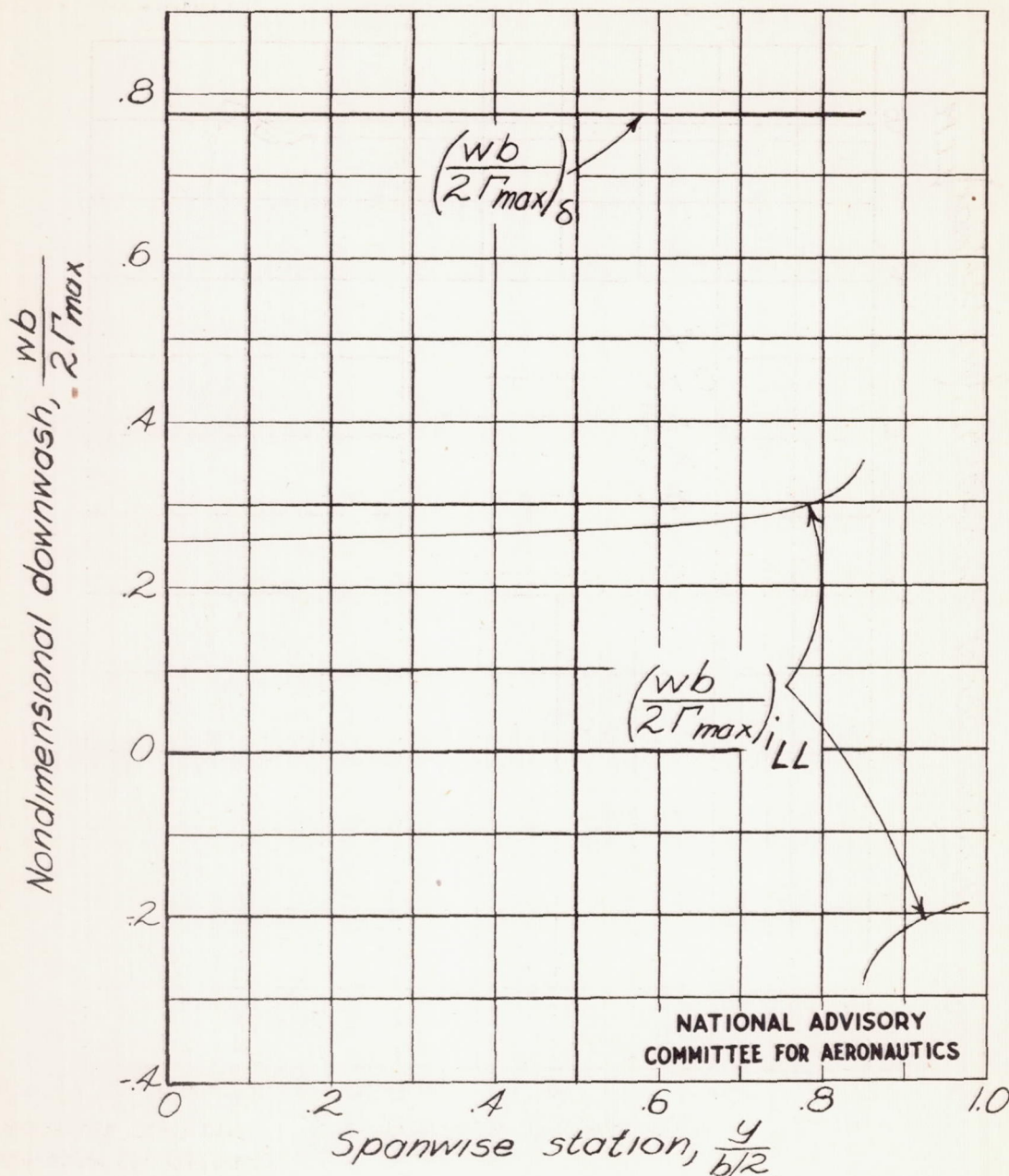


Figure 7 - Values of the nondimensional downwash parameters $(wb/2\Gamma_{max})_s$ and $(wb/2\Gamma_{max})_{iLL}$ calculated for a thin elliptic wing of aspect ratio 3 with a 0.5-chord elevator. Lifting-line-theory loading of figure 1.

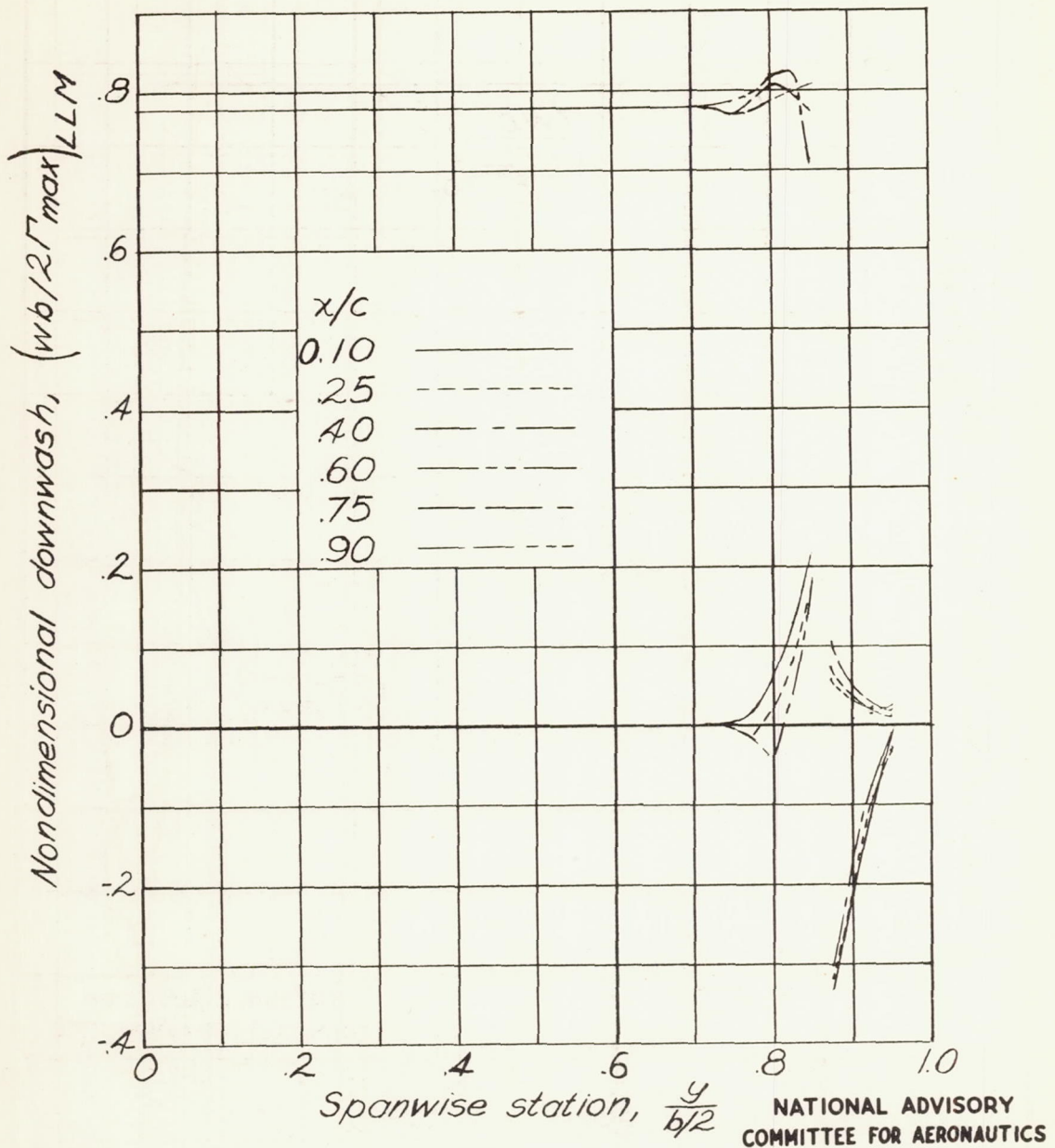


Figure 8.- The nondimensional downwash $(wb/2\Gamma_{max})_{LLM}$ calculated by the two-dimensional theories for a thin elliptic wing of aspect ratio 3 with a 0.5-chord 0.85-span plain flap. Modified lifting-line-theory loading of figure 3.

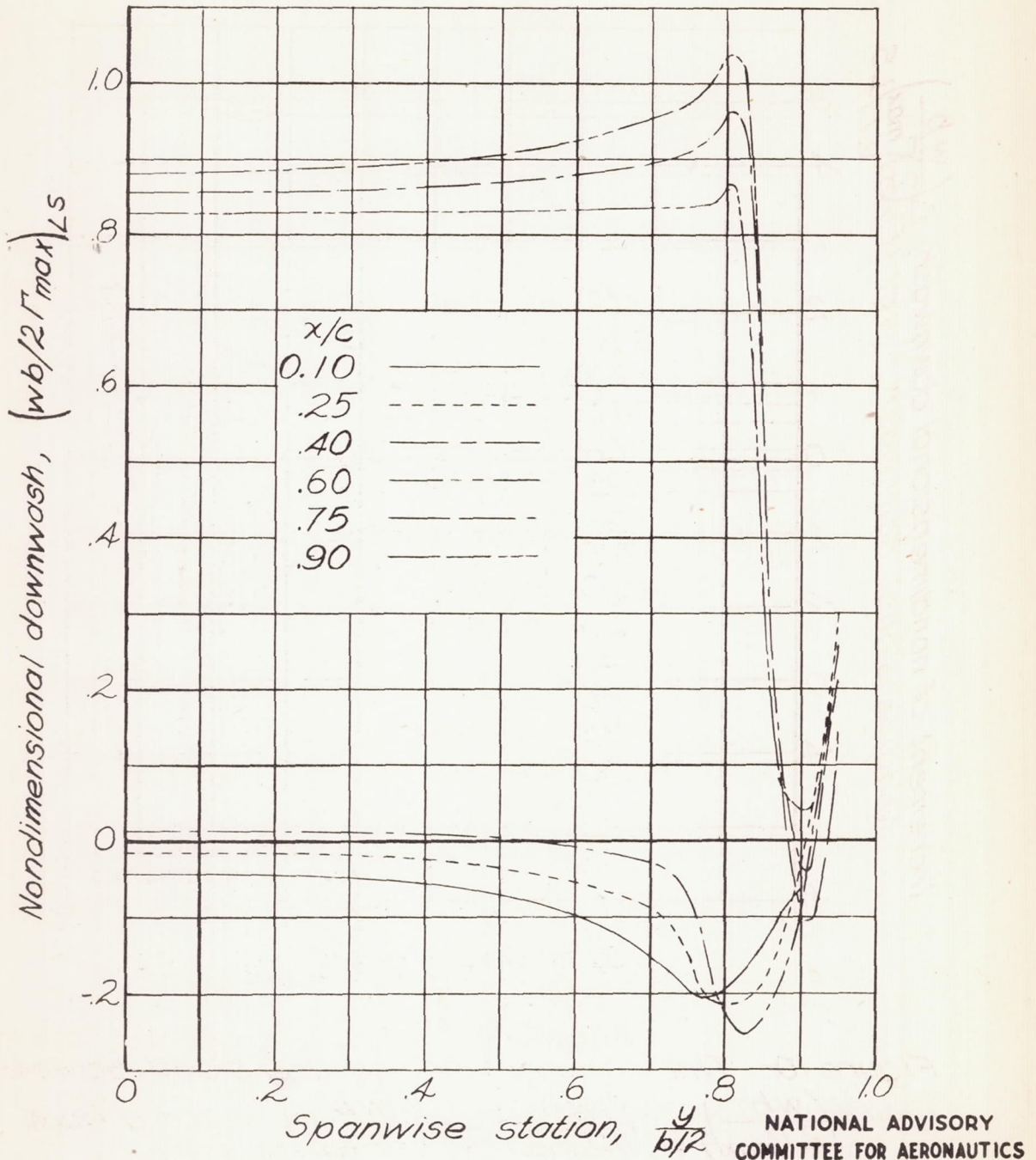


Figure 9.- The nondimensional downwash $(wb/2\Gamma_{max})_{LS}$ determined from the electromagnetic-analogy model of figure 6 for a thin elliptic wing of aspect ratio 3 with a 0.5-chord 0.85-span plain elevator.

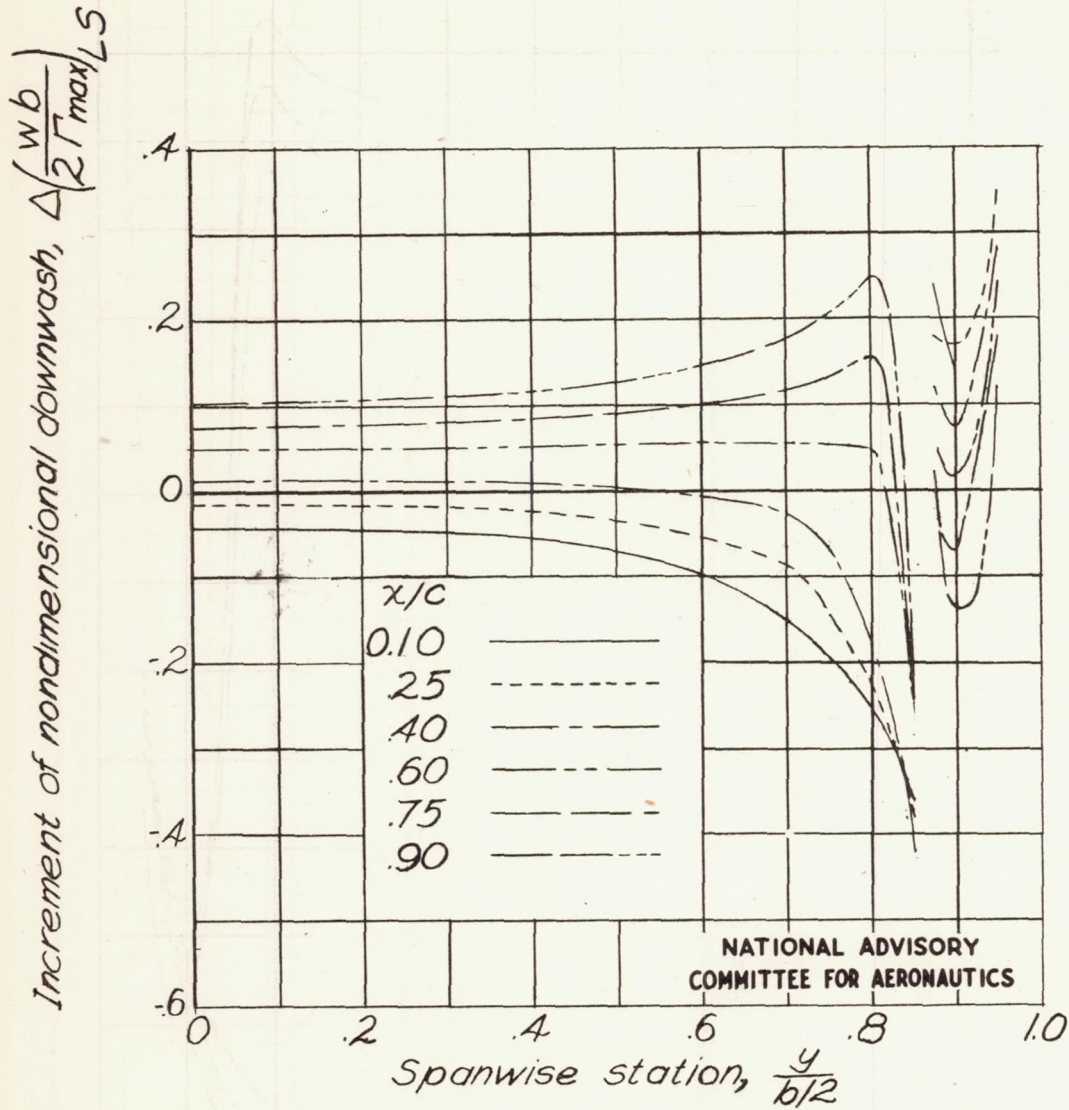


Figure 10- The increment of nondimensional downwash $\Delta\left(\frac{wb}{2\Gamma_{max}LS}\right) = \left(\frac{wb}{2\Gamma_{max}LS}\right) - \left(\frac{wb}{2\Gamma_{max}LLM}\right)$ for a thin elliptic wing of aspect ratio 3 with a 0.5-chord 0.85-span plain elevator.

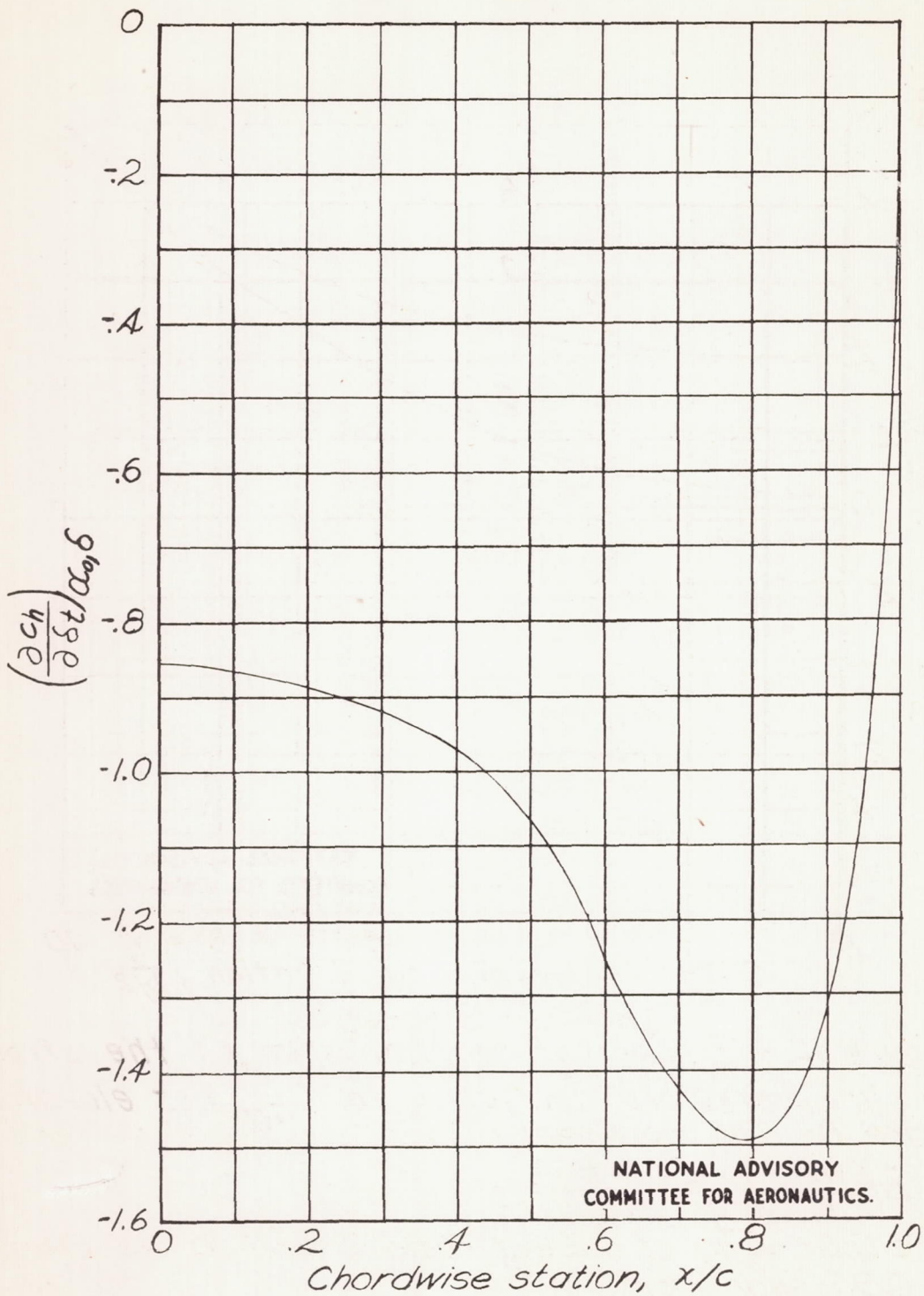


Figure 11.- Variation of parameter $(\frac{\partial ch}{\partial \delta t})\alpha_{0,\delta}$ with chordwise location of tab hinge for a 0.5-chord plain flap determined from thin-airfoil theory.

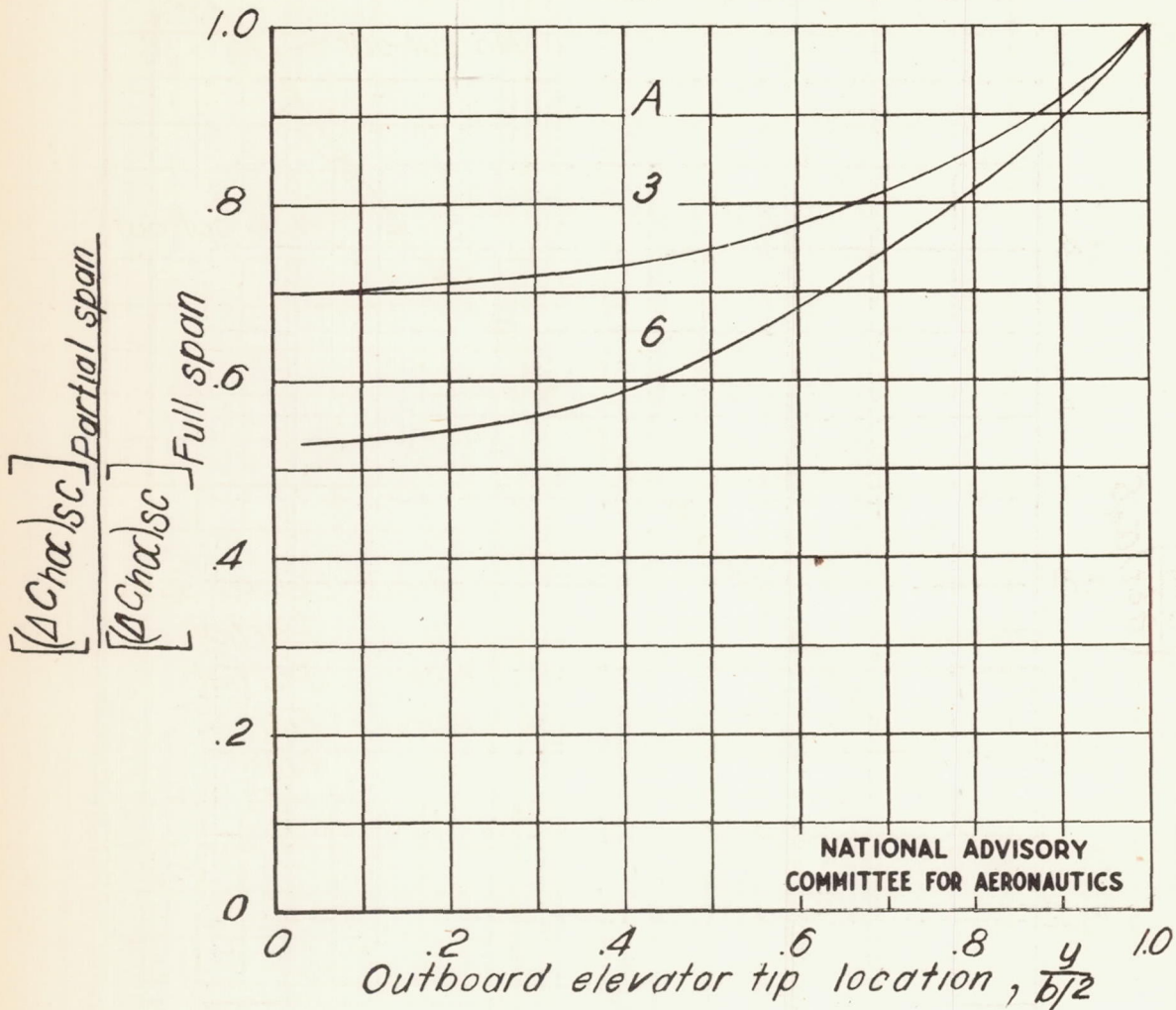
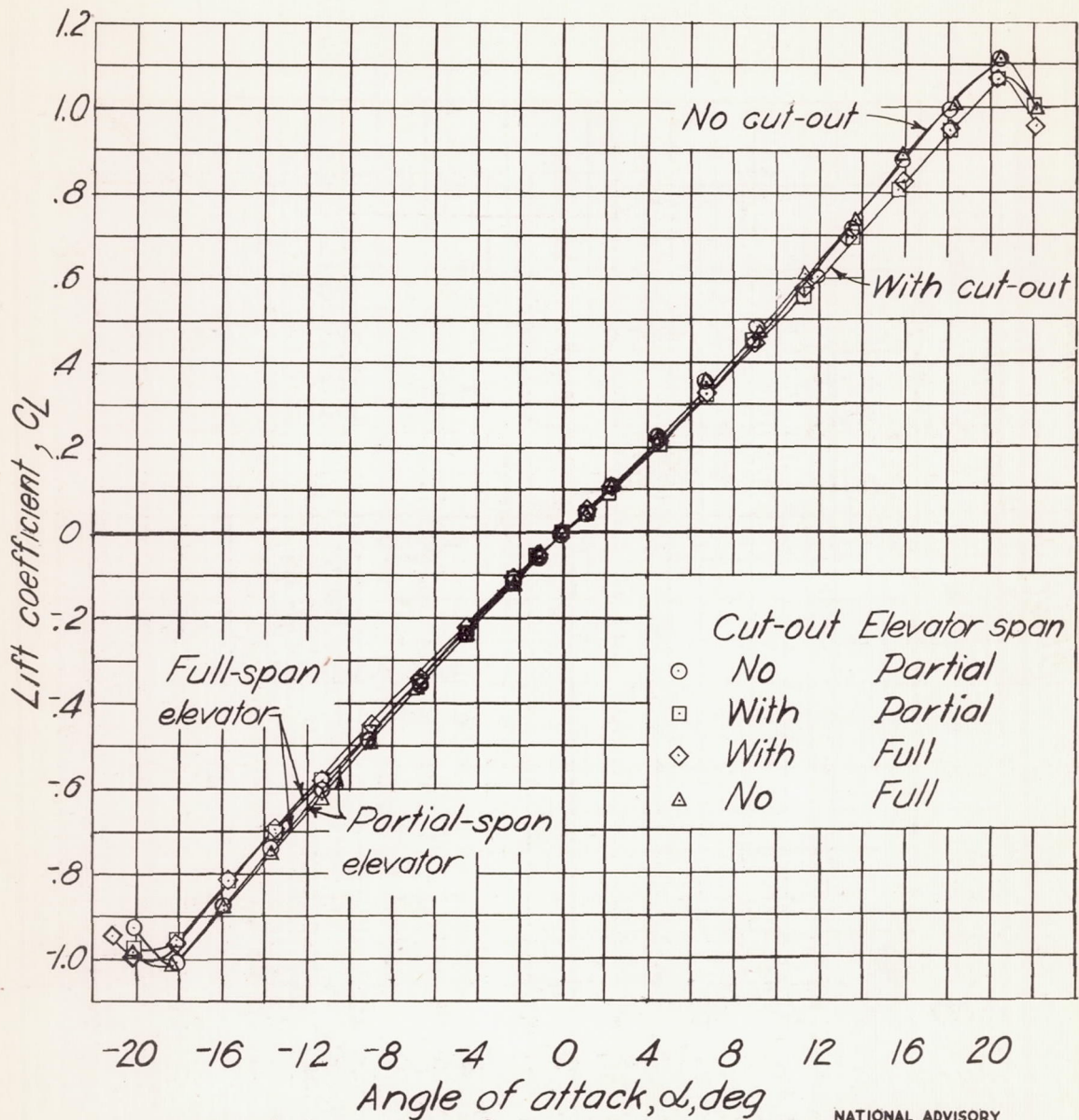
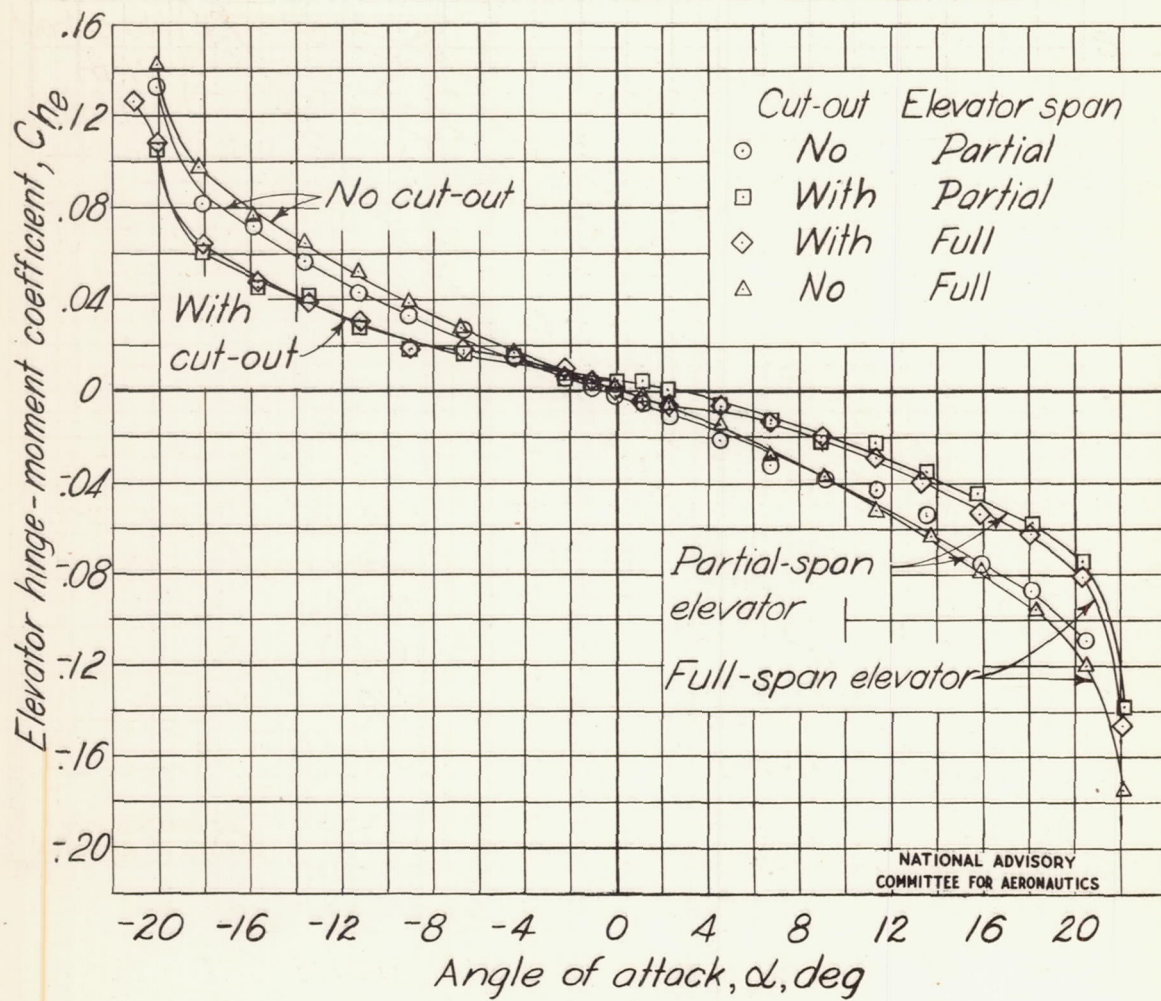


Figure 12.- Effect of partial span on the stream-line-curvature correction to $C_{h\alpha}$ for elevators.



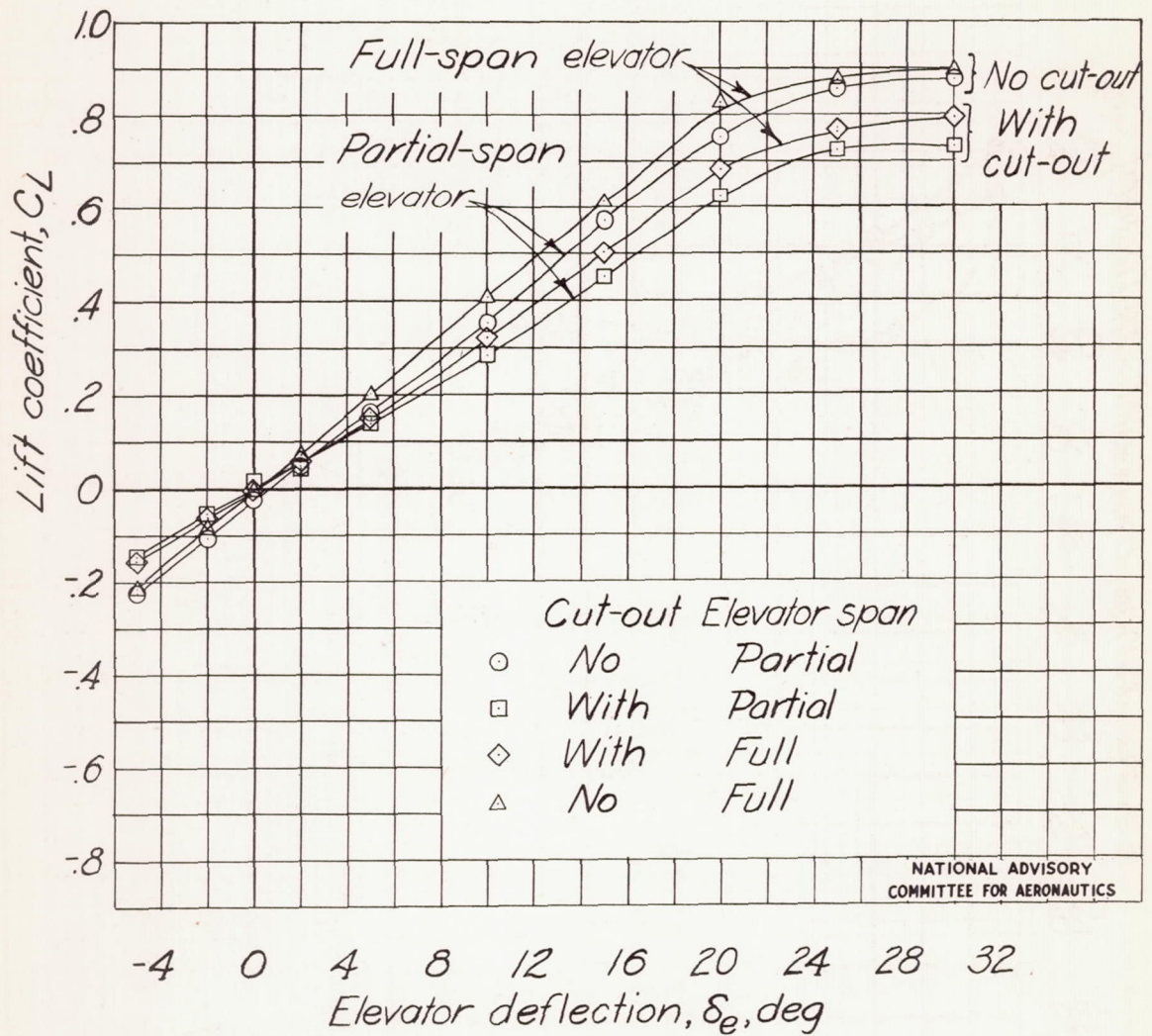
NATIONAL ADVISORY
COMMITTEE FOR AERONAUTICS

Figure 13.-Aerodynamic characteristics of an elliptic semi-span horizontal tail surface with a partial- and full-span $0.50c$ plain elevator and with and without cut-out. $q = 13$ pounds per square foot; $A = 3$.



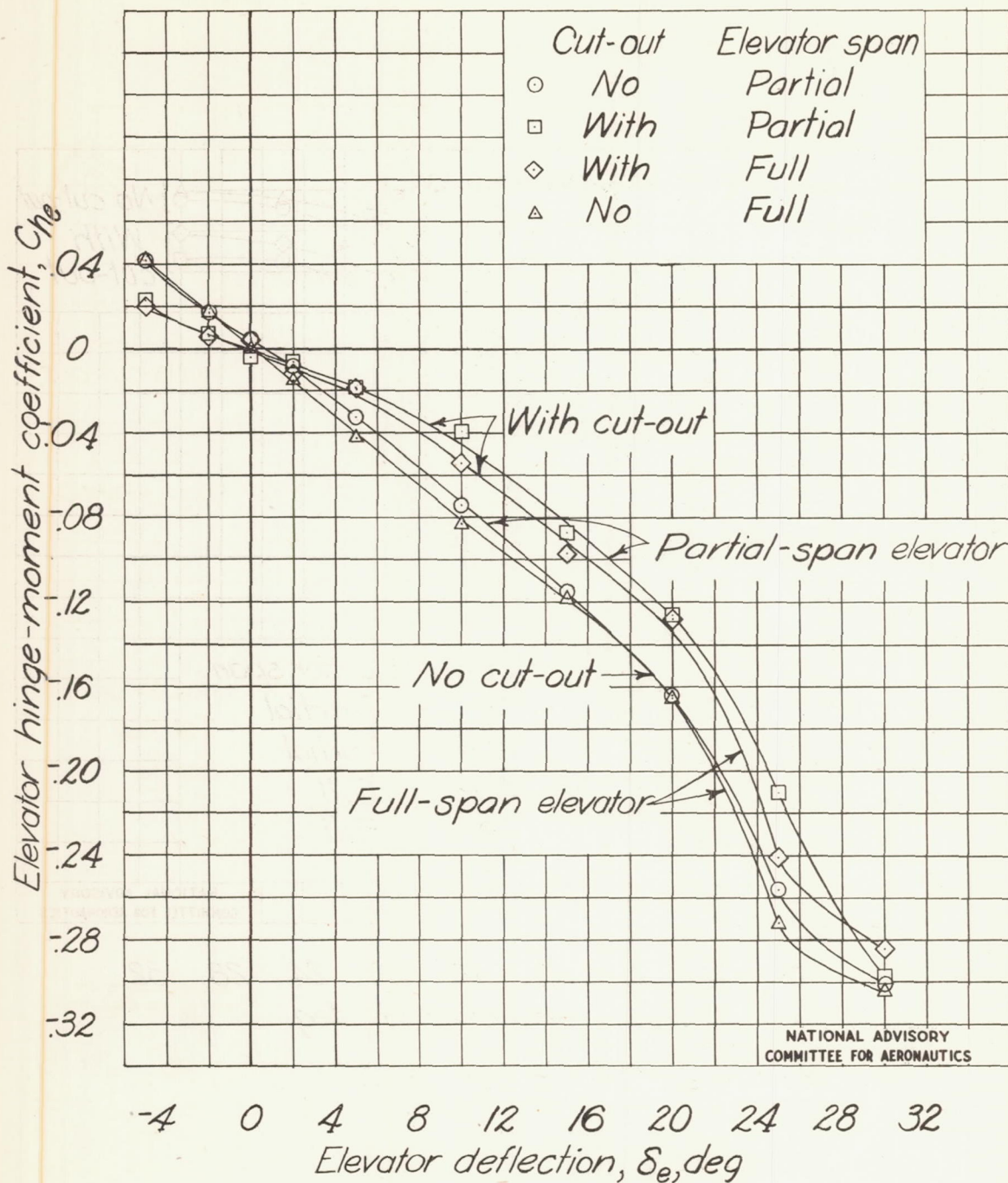
(a) Continued. Sealed gap; $\delta_e = 0^\circ$.

Figure 13.-Continued.



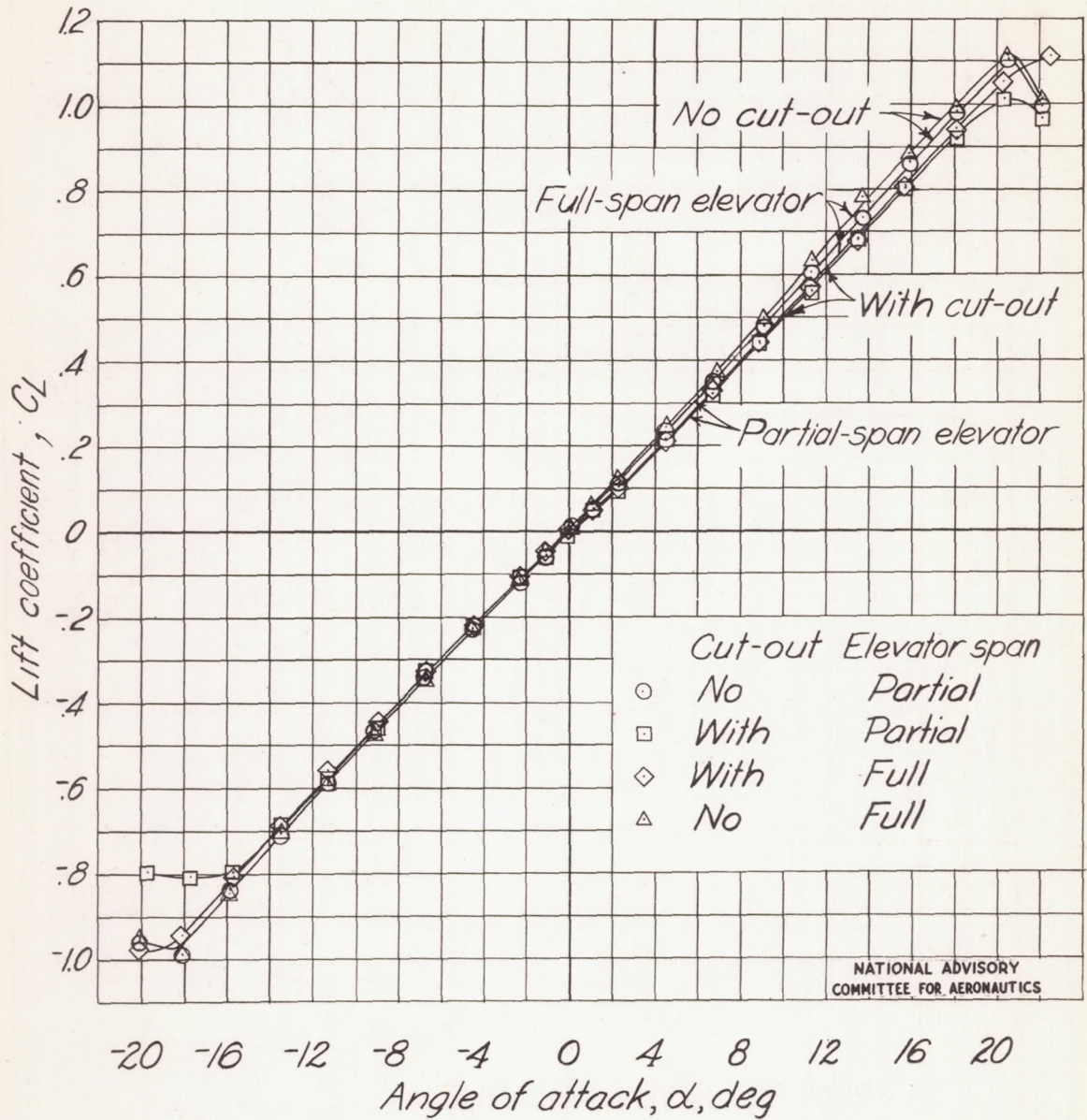
(a) Continued. Sealed gap; $\alpha = 0^\circ$

Figure 13.-Continued.

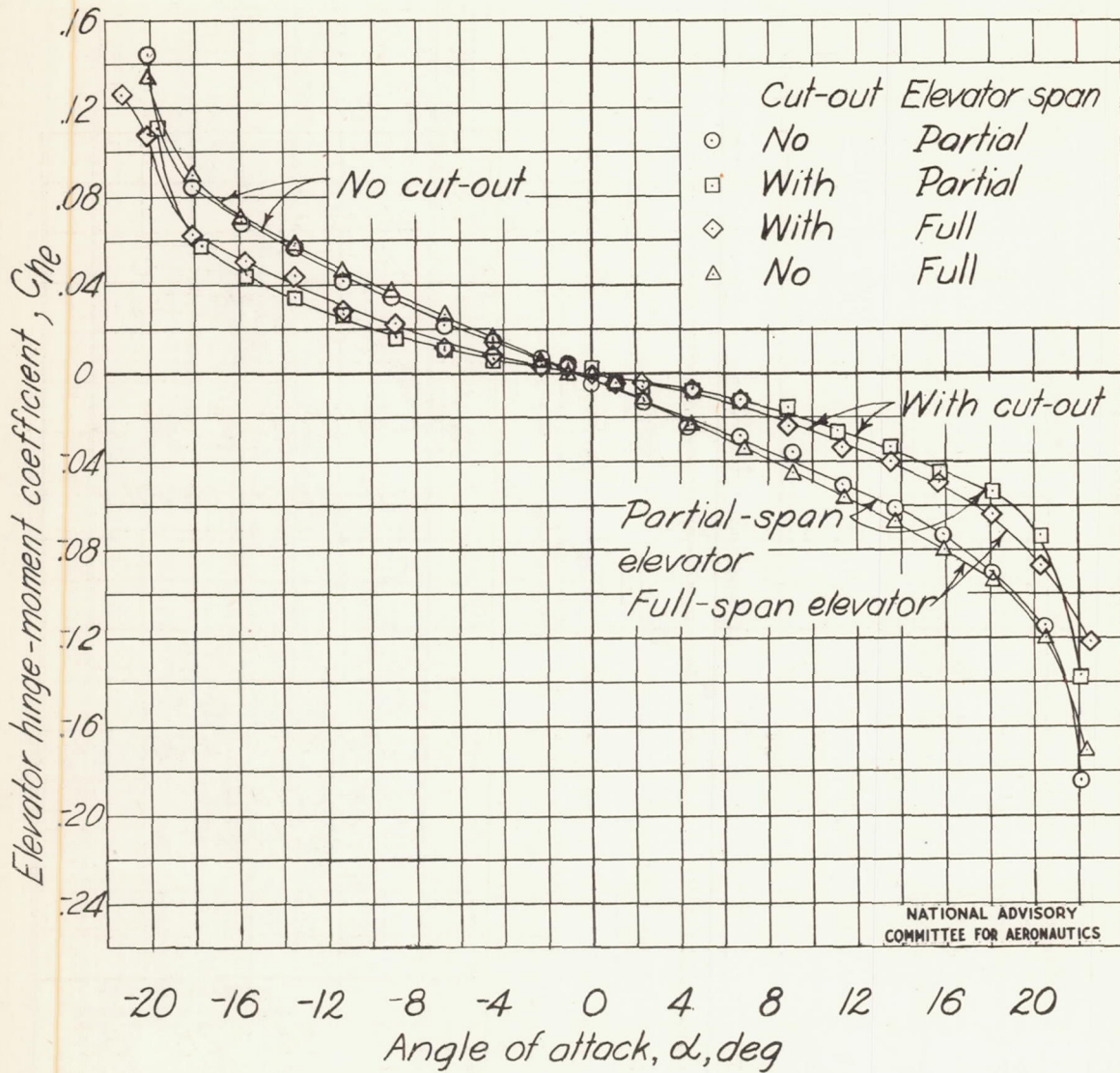


(a) Concluded. Sealed gap; $\alpha = 0^\circ$

Figure 13.-Continued.

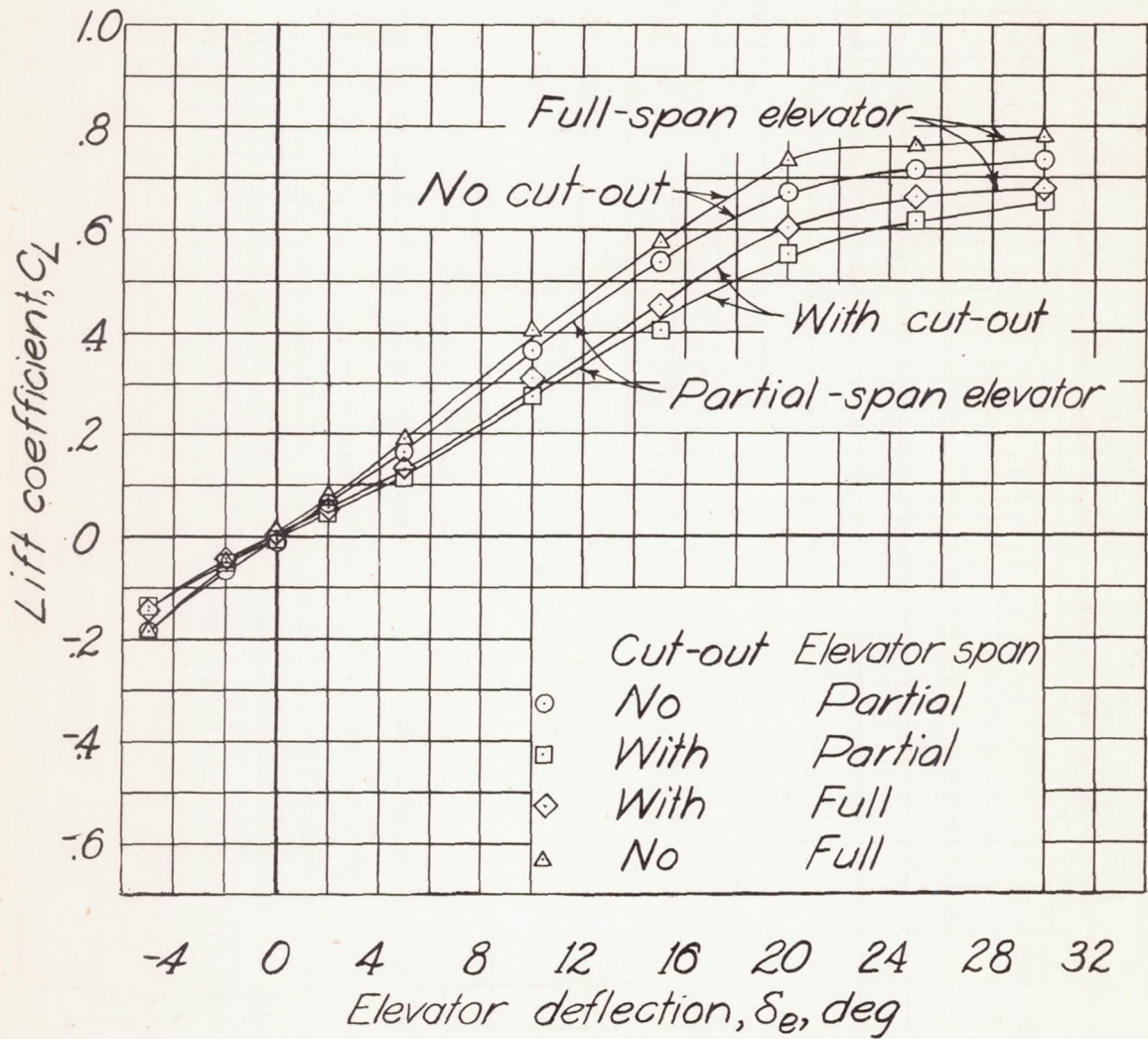


(b) $0.005c$ gap; $\delta_e = 0^\circ$.
 Figure 13. -Continued.



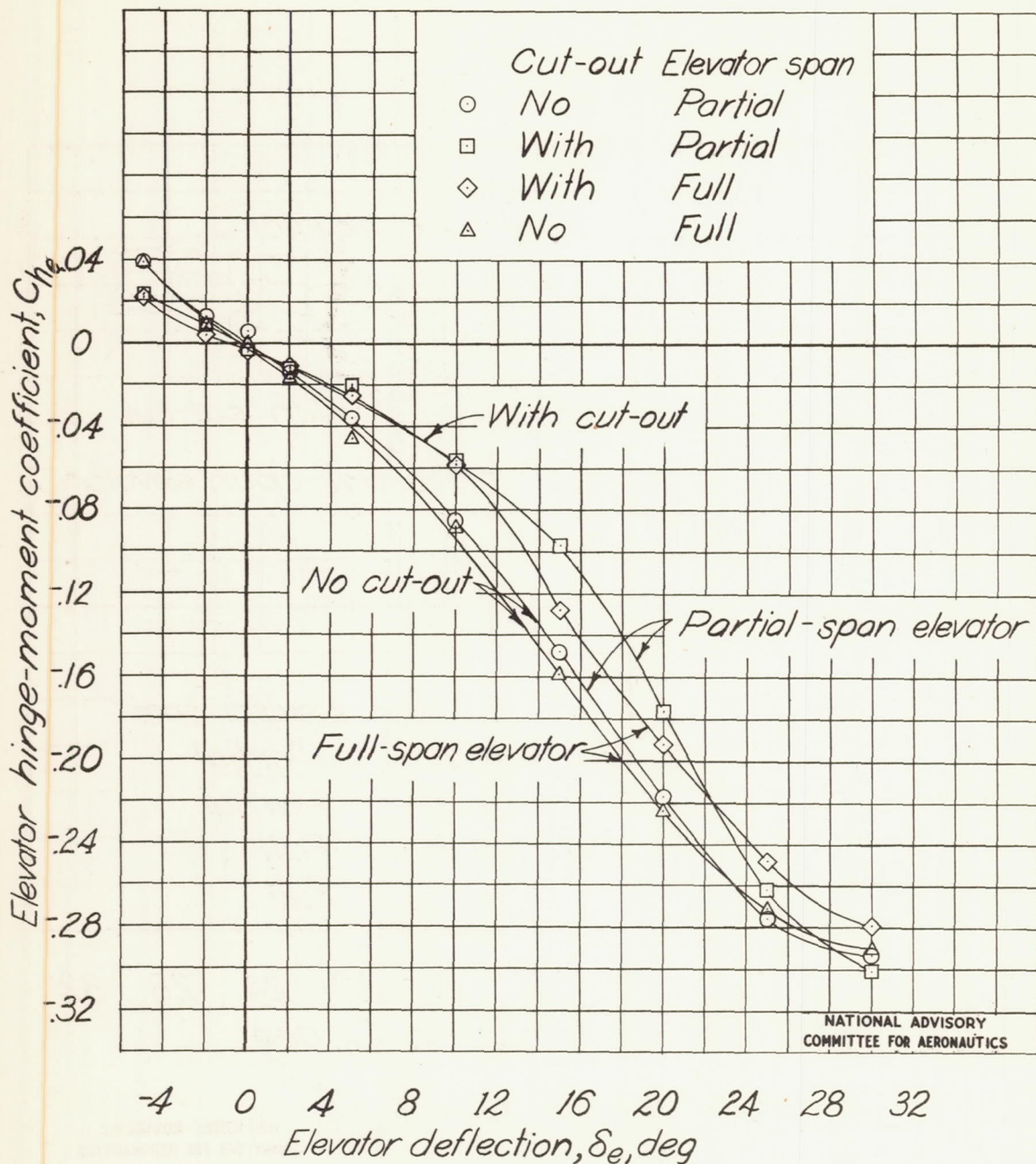
(b) Continued. $0.005c$ gap; $\delta_e = 0^\circ$.

Figure 13.-Continued.



(b) Continued. 0.005c gap; $\alpha = 0^\circ$

Figure 13.-Continued.



(b) Concluded. 0.005c gap; $\alpha = 0^\circ$.

Figure 13.-Concluded.

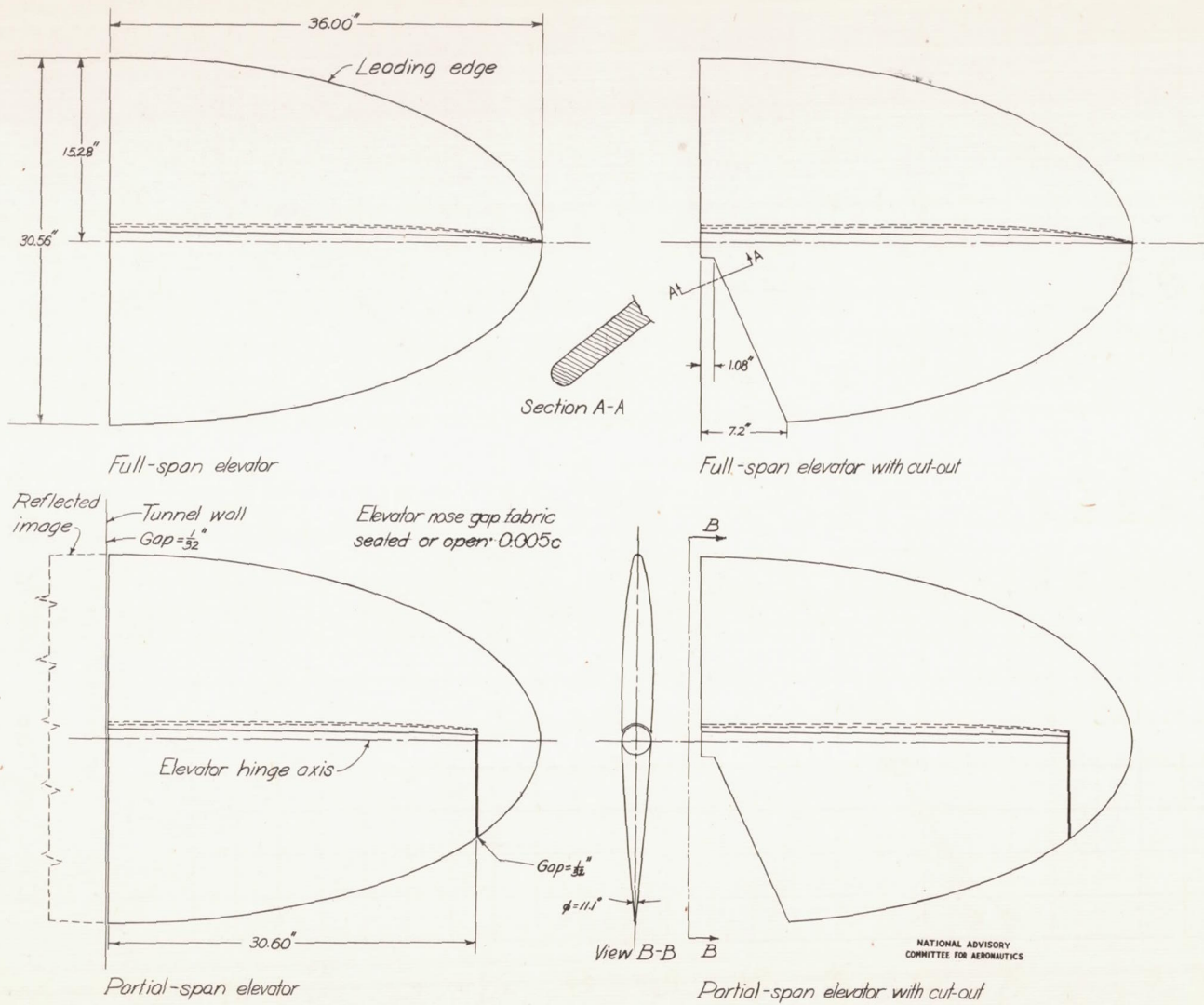


Figure 14. - Details of an elliptic semispan horizontal tail surface with a partial and full-span 0.50c plain elevator with and without cut-out. NACA 0009 section; Aspect ratio = 3; area = 6 square feet without cut-out, 5.60 square feet with cut-out.

